

## COMBINATORICS OF KP SOLITONS FROM THE REAL GRASSMANNIAN

YUJI KODAMA AND LAUREN WILLIAMS

ABSTRACT. Given a point  $A$  in the real Grassmannian, it is well-known that one can construct a soliton solution  $u_A(x, y, t)$  to the KP equation. The *contour plot* of such a solution provides a tropical approximation to the solution when the variables  $x$ ,  $y$ , and  $t$  are considered on a large scale and the time  $t$  is fixed. In this paper we give an overview of our work on the combinatorics of such contour plots. Using the positroid stratification and the Deodhar decomposition of the Grassmannian (and in particular the combinatorics of *Go-diagrams*), we completely describe the asymptotics of these contour plots when  $y$  or  $t$  go to  $\pm\infty$ . Other highlights include: a surprising connection with total positivity and cluster algebras; results on the *inverse problem*; and the characterization of regular soliton solutions – that is, a soliton solution  $u_A(x, y, t)$  is regular for all times  $t$  if and only if  $A$  comes from the *totally non-negative part* of the Grassmannian.

Arrangements of stones  
reveal patterns in the waves  
as space-time expands



とき超えて  
碁石が証す  
波文様

## CONTENTS

1. Introduction	1
2. Background on the Grassmannian and its totally non-negative part	3
3. A Deodhar decomposition of the Grassmannian	6
4. Deodhar components in the Grassmannian and Go-diagrams	9
5. Soliton solutions to the KP equation and their contour plots	12
6. Unbounded line-solitons at $y \gg 0$ and $y \ll 0$	15
7. Soliton graphs and generalized plabic graphs	17
8. The contour plot for $t \ll 0$	18
9. Total positivity, regularity, and cluster algebras	21
10. The inverse problem for soliton graphs	25
References	26

## 1. INTRODUCTION

The main purpose of this paper is to give an exposition of our recent work [18, 19, 20], which found surprising connections between soliton solutions of the KP equation and the combinatorics of the real Grassmannian. The KP equation is a two-dimensional nonlinear dispersive wave equation which was

*Date:* May 28, 2018.

The first author was partially supported by NSF grants DMS-0806219 and DMS-1108813. The second author was partially supported by an NSF CAREER award and an Alfred Sloan Fellowship.

proposed by Kadomtsev and Pevniashvili in 1970 to study the stability problem of the soliton solution of the Korteweg-de Vries (KdV) equation [13]. The equation has a rich mathematical structure, and is now considered to be the prototype of an integrable nonlinear dispersive wave equation with two spatial dimensions (see for example [24, 1, 9, 23, 12]). The KP equation can also be used to describe shallow water wave phenomena, including resonant interactions.

An important breakthrough in the KP theory was made by Sato [26], who realized that solutions of the KP equation could be written in terms of points on an infinite-dimensional Grassmannian. The present paper, which gives an overview of most of our results of [19] and [20], deals with a real, finite-dimensional version of the Sato theory. In particular, we are interested in *soliton solutions*, that is, solutions that are localized along certain rays in the  $xy$  plane called *line-solitons*. Such a solution can be constructed from a point  $A$  of the real Grassmannian. More specifically, one can apply the *Wronskian form* [26, 27, 11, 12] to  $A$  to produce a certain sum of exponentials called a  $\tau$ -function  $\tau_A(x, y, t)$ , and from the  $\tau$ -function one can construct a solution  $u_A(x, y, t)$  to the KP equation.

Recently several authors have studied the soliton solutions  $u_A(x, y, t)$  which come from points  $A$  of the *totally non-negative part of the Grassmannian*  $(Gr_{k,n})_{\geq 0}$ , that is, those points of the real Grassmannian  $Gr_{k,n}$  whose Plücker coordinates are all non-negative [3, 16, 2, 5, 7, 18, 19]. These solutions are *regular*, and include a large variety of soliton solutions which were previously overlooked by those using the Hirota method of a perturbation expansion [12].

A main goal of [20] was to understand the soliton solutions  $u_A(x, y, t)$  coming from arbitrary points  $A$  of the real Grassmannian, not just the totally non-negative part. In general such solutions are no longer regular – they may have singularities along rays in the  $xy$  plane – but it is possible, nevertheless, to understand a great deal about the asymptotics of such solutions, when the absolute value of the spatial variable  $y$  goes to infinity, and also when the absolute value of the time variable  $t$  goes to infinity.

Two related decompositions of the real Grassmannian are useful for understanding the asymptotics of soliton solutions  $u_A(x, y, t)$ . The first is Postnikov’s *positroid stratification* of the Grassmannian [25], whose strata are indexed by various combinatorial objects including decorated permutations and  $\mathbb{J}$ -diagrams. This decomposition determines the asymptotics of soliton solutions when  $|y| \gg 0$ , and our results here extend work of [2, 5, 7, 18, 19] from the setting of the non-negative part of the Grassmannian to the entire real Grassmannian. The second decomposition, which we call the *Deodhar decomposition* [20], is the projection to the Grassmannian of a decomposition of the flag variety due to Deodhar. The Deodhar decomposition refines the positroid stratification, and its components may be indexed by certain tableaux filled with black and white stones called *Go-diagrams*, which generalize  $\mathbb{J}$ -diagrams. This decomposition determines the asymptotics of soliton solutions when  $|t| \gg 0$ . More specifically, it allows us to compute the *contour plots* at  $|t| \gg 0$  of such solitons, which are tropical approximations to the solution when  $x$ ,  $y$ , and  $t$  are on a large scale [20].

By using our results on the asymptotics of soliton solutions when  $t \ll 0$ , one may give a characterization of the regular soliton solutions coming from the real Grassmannian. More specifically, a soliton solution  $u_A(x, y, t)$  coming from a point  $A$  of the real Grassmannian is regular for all times  $t$  if and only if  $A$  is a point of the totally non-negative part of the Grassmannian [20].

The regularity theorem above provides an important motivation for studying soliton solutions coming from  $(Gr_{k,n})_{\geq 0}$ . Indeed, as we showed in [19], such soliton solutions have an even richer combinatorial structure than those coming from  $Gr_{k,n}$ . For example, (generic) contour plots coming from the totally positive part  $(Gr_{k,n})_{> 0}$  of the Grassmannian give rise to *clusters* for the cluster algebra associated to the Grassmannian. And up to a combinatorial equivalence, the contour plots coming from  $(Gr_{2,n})_{> 0}$  are in bijection with triangulations of an  $n$ -gon. Finally, if either  $A \in (Gr_{k,n})_{> 0}$ , or  $A \in (Gr_{k,n})_{\geq 0}$  and  $t \ll 0$ , then one may solve the *inverse problem* for  $u_A(x, y, t)$ : that is, given the contour plot  $\mathcal{C}_t(u_A)$  and the time  $t$ , one may reconstruct the element  $A \in (Gr_{k,n})_{\geq 0}$ . And therefore one may reconstruct the entire evolution of this soliton solution over time [19].

The structure of this paper is as follows. In Section 2 we provide background on the Grassmannian and some of its decompositions, including the positroid stratification. In Section 3 we describe the Deodhar decomposition of the complete flag variety and its projection to the Grassmannian, while in Section 4 we explain how to index Deodhar components in the Grassmannian by *Go-diagrams*. Subsequent sections provide applications of the previous results to soliton solutions of the KP equation. In Section 5 we explain how to produce a soliton solution to the KP equation from a point of the real Grassmannian, and then define the *contour plot* associated to a soliton solution at a fixed time  $t$ . In Section 6 we use the positroid stratification to describe the unbounded line-solitons in contour plots of soliton solutions at  $y \gg 0$  and  $y \ll 0$ . In Section 7 we define the more combinatorial notions of *soliton graph* and *generalized plabic graph*. In Section 8 we use the Deodhar decomposition to describe contour plots of soliton solutions for  $t \ll 0$ . In Section 9 we describe the significance of total positivity to soliton solutions, by discussing the regularity problem, as well as the connection to cluster algebras. Finally in Section 10, we give results on the inverse problem for soliton solutions coming from  $(Gr_{k,n})_{\geq 0}$ .

## 2. BACKGROUND ON THE GRASSMANNIAN AND ITS TOTALLY NON-NEGATIVE PART

The *real Grassmannian*  $Gr_{k,n}$  is the space of all  $k$ -dimensional subspaces of  $\mathbb{R}^n$ . An element of  $Gr_{k,n}$  can be viewed as a full-rank  $k \times n$  matrix modulo left multiplication by nonsingular  $k \times k$  matrices. In other words, two  $k \times n$  matrices represent the same point in  $Gr_{k,n}$  if and only if they can be obtained from each other by row operations. Let  $\binom{[n]}{k}$  be the set of all  $k$ -element subsets of  $[n] := \{1, \dots, n\}$ . For  $I \in \binom{[n]}{k}$ , let  $\Delta_I(A)$  be the *Plücker coordinate*, that is, the maximal minor of the  $k \times n$  matrix  $A$  located in the column set  $I$ . The map  $A \mapsto (\Delta_I(A))$ , where  $I$  ranges over  $\binom{[n]}{k}$ , induces the *Plücker embedding*  $Gr_{k,n} \hookrightarrow \mathbb{RP}^{\binom{n}{k}-1}$ . The *totally non-negative part of the Grassmannian*  $(Gr_{k,n})_{\geq 0}$  is the subset of  $Gr_{k,n}$  such that all Plücker coordinates are non-negative.

We now describe several useful decompositions of the Grassmannian: the matroid stratification, the Schubert decomposition, and the positroid stratification. When one restricts the positroid stratification to  $(Gr_{k,n})_{\geq 0}$ , one gets a cell decomposition of  $(Gr_{k,n})_{\geq 0}$  into *positroid cells*.

### 2.1. The matroid stratification of $Gr_{k,n}$ .

*Definition 2.1.* A *matroid* of rank  $k$  on the set  $[n]$  is a nonempty collection  $\mathcal{M} \subset \binom{[n]}{k}$  of  $k$ -element subsets in  $[n]$ , called *bases* of  $\mathcal{M}$ , that satisfies the *exchange axiom*: For any  $I, J \in \mathcal{M}$  and  $i \in I$  there exists  $j \in J$  such that  $(I \setminus \{i\}) \cup \{j\} \in \mathcal{M}$ .

Given an element  $A \in Gr_{k,n}$ , there is an associated matroid  $\mathcal{M}_A$  whose bases are the  $k$ -subsets  $I \subset [n]$  such that  $\Delta_I(A) \neq 0$ .

*Definition 2.2.* Let  $\mathcal{M} \subset \binom{[n]}{k}$  be a matroid. The *matroid stratum*  $S_{\mathcal{M}}$  is defined to be

$$S_{\mathcal{M}} = \{A \in Gr_{k,n} \mid \Delta_I(A) \neq 0 \text{ if and only if } I \in \mathcal{M}\}.$$

This gives a stratification of  $Gr_{k,n}$  called the *matroid stratification*, or *Gelfand-Serganova stratification*. The matroids  $\mathcal{M}$  with nonempty strata  $S_{\mathcal{M}}$  are called *realizable* over  $\mathbb{R}$ .

**2.2. The Schubert decomposition of  $Gr_{k,n}$ .** Recall that the partitions  $\lambda \subset (n-k)^k$  are in bijection with  $k$ -element subset  $I \subset [n]$ . The boundary of the Young diagram of such a partition  $\lambda$  forms a lattice path from the upper-right corner to the lower-left corner of the rectangle  $(n-k)^k$ . Let us label the  $n$  steps in this path by the numbers  $1, \dots, n$ , and define  $I = I(\lambda)$  as the set of labels on the  $k$  vertical steps in the path. Conversely, we let  $\lambda(I)$  denote the partition corresponding to the subset  $I$ .

*Definition 2.3.* For each partition  $\lambda \subset (n-k)^k$ , one can define the *Schubert cell*  $\Omega_{\lambda}$  by

$$\Omega_{\lambda} = \{A \in Gr_{k,n} \mid I(\lambda) \text{ is the lexicographically minimal base of } \mathcal{M}_A\}.$$

As  $\lambda$  ranges over the partitions contained in  $(n-k)^k$ , this gives the *Schubert decomposition* of the Grassmannian  $Gr_{k,n}$ , i.e.

$$Gr_{k,n} = \bigsqcup_{\lambda \subset (n-k)^k} \Omega_\lambda.$$

We now define the *shifted linear order*  $<_i$  (for  $i \in [n]$ ) to be the total order on  $[n]$  defined by

$$i <_i i+1 <_i i+2 <_i \cdots <_i n <_i 1 <_i \cdots <_i i-1.$$

One can then define *cyclically shifted Schubert cells* as follows.

*Definition 2.4.* For each partition  $\lambda \subset (n-k)^k$  and  $i \in [n]$ , the *cyclically shifted Schubert cell*  $\Omega_\lambda^i$  is

$$\Omega_\lambda^i = \{A \in Gr_{k,n} \mid I(\lambda) \text{ is the lexicographically minimal base of } \mathcal{M}_A \text{ with respect to } <_i\}.$$

**2.3. The positroid stratification of  $Gr_{k,n}$ .** The *positroid stratification* of the real Grassmannian  $Gr_{k,n}$  is obtained by taking the simultaneous refinement of the  $n$  Schubert decompositions with respect to the  $n$  shifted linear orders  $<_i$ . This stratification was first considered by Postnikov [25], who showed that the strata are conveniently described in terms of *Grassmann necklaces*, as well as *decorated permutations*, (equivalence classes of) *plabic graphs*, and  $\mathfrak{J}$ -*diagrams*. Postnikov coined the terminology *positroid* because the intersection of the positroid stratification with  $(Gr_{k,n})_{\geq 0}$  gives a cell decomposition of  $(Gr_{k,n})_{\geq 0}$  (whose cells are called *positroid cells*).

*Definition 2.5.* [25, Definition 16.1] A *Grassmann necklace* is a sequence  $\mathcal{I} = (I_1, \dots, I_n)$  of subsets  $I_r \subset [n]$  such that, for  $i \in [n]$ , if  $i \in I_i$  then  $I_{i+1} = (I_i \setminus \{i\}) \cup \{j\}$ , for some  $j \in [n]$ ; and if  $i \notin I_i$  then  $I_{i+1} = I_i$ . (Here indices  $i$  are taken modulo  $n$ .) In particular, we have  $|I_1| = \cdots = |I_n|$ , which is equal to some  $k \in [n]$ . We then say that  $\mathcal{I}$  is a Grassmann necklace of *type*  $(k, n)$ .

*Example 2.6.* (1257, 2357, 3457, 4567, 5678, 6789, 1789, 1289, 1259) is a Grassmann necklace of type (4, 9).

*Lemma 2.7.* [25, Lemma 16.3] Given  $A \in Gr_{k,n}$ , let  $\mathcal{I}(A) = (I_1, \dots, I_n)$  be the sequence of subsets in  $[n]$  such that, for  $i \in [n]$ ,  $I_i$  is the lexicographically minimal subset of  $\binom{[n]}{k}$  with respect to the shifted linear order  $<_i$  such that  $\Delta_{I_i}(A) \neq 0$ . Then  $\mathcal{I}(A)$  is a Grassmann necklace of type  $(k, n)$ .

If  $A$  is in the matroid stratum  $S_{\mathcal{M}}$ , we also use  $\mathcal{I}_{\mathcal{M}}$  to denote the sequence  $(I_1, \dots, I_n)$  defined above. This leads to the following description of the *positroid stratification* of  $Gr_{k,n}$ .

*Definition 2.8.* Let  $\mathcal{I} = (I_1, \dots, I_n)$  be a Grassmann necklace of type  $(k, n)$ . The *positroid stratum*  $S_{\mathcal{I}}$  is defined to be

$$\begin{aligned} S_{\mathcal{I}} &= \{A \in Gr_{k,n} \mid \mathcal{I}(A) = \mathcal{I}\} \\ &= \bigcap_{i=1}^n \Omega_{\lambda^{(I_i)}}^i. \end{aligned}$$

The second equality follows from Definition 2.8 and Definition 2.4. Note that each positroid stratum is an intersection of  $n$  cyclically shifted Schubert cells.

*Definition 2.9.* [25, Definition 13.3] A *decorated permutation*  $\pi = (\pi, col)$  is a permutation  $\pi \in S_n$  together with a coloring function  $col$  from the set of fixed points  $\{i \mid \pi(i) = i\}$  to  $\{1, -1\}$ . So a decorated permutation is a permutation with fixed points colored in one of two colors. A *weak excedance* of  $\pi$  is a pair  $(i, \pi_i)$  such that either  $\pi(i) > i$ , or  $\pi(i) = i$  and  $col(i) = 1$ . We call  $i$  the *weak excedance position*. If  $\pi(i) > i$  (respectively  $\pi(i) < i$ ) then  $(i, \pi_i)$  is called an excedance (respectively, nonexcedance).

*Example 2.10.* The decorated permutation (written in one-line notation) (6, 7, 1, 2, 8, 3, 9, 4, 5) has no fixed points, and four weak excedances, in positions 1, 2, 5 and 7.

*Definition 2.11.* A *plabic graph* is a planar undirected graph  $G$  drawn inside a disk with  $n$  *boundary vertices*  $1, \dots, n$  placed in counterclockwise order around the boundary of the disk, such that each boundary vertex  $i$  is incident to a single edge.<sup>1</sup> Each internal vertex is colored black or white. See the left of Figure 1 for an example.

*Definition 2.12.* [25, Definition 6.1] Fix  $k, n$ . If  $\lambda$  is a partition, let  $Y_\lambda$  denote its Young diagram. A  $\mathbb{J}$ -*diagram*  $(\lambda, D)_{k,n}$  of type  $(k, n)$  is a partition  $\lambda$  contained in a  $k \times (n - k)$  rectangle together with a filling  $D : Y_\lambda \rightarrow \{0, +\}$  which has the  $\mathbb{J}$ -*property*: there is no 0 which has a + above it and a + to its left.<sup>2</sup> (Here, “above” means above and in the same column, and “to its left” means to the left and in the same row.) See the right of Figure 1 for an example.

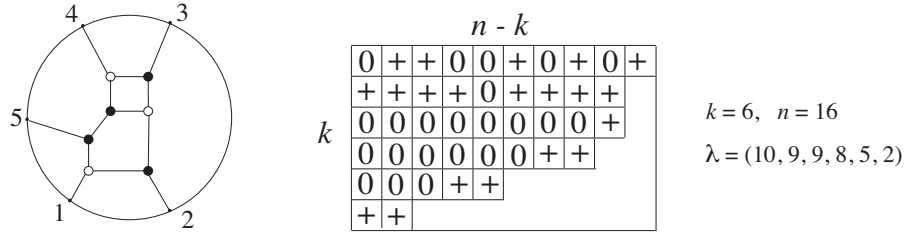


FIGURE 1. A plabic graph and a Le-diagram  $L = (\lambda, D)_{k,n}$ .

We now review some of the bijections among these objects.

*Definition 2.13.* [25, Section 16] Given a Grassmann necklace  $\mathcal{I}$ , define a decorated permutation  $\pi^\cdot = \pi^\cdot(\mathcal{I})$  by requiring that

- (1) if  $I_{i+1} = (I_i \setminus \{i\}) \cup \{j\}$ , for  $j \neq i$ , then  $\pi^\cdot(j) = i$ .<sup>3</sup>
- (2) if  $I_{i+1} = I_i$  and  $i \in I_i$  then  $\pi^\cdot(i) = i$  is colored with  $col(i) = 1$ .
- (3) if  $I_{i+1} = I_i$  and  $i \notin I_i$  then  $\pi^\cdot(i) = i$  is colored with  $col(i) = -1$ .

As before, indices are taken modulo  $n$ .

If  $\pi^\cdot = \pi^\cdot(\mathcal{I})$ , then we also use the notation  $S_{\pi^\cdot}$  to refer to the positroid stratum  $S_{\mathcal{I}}$ .

*Example 2.14.* Definition 2.13 carries the Grassmann necklace of Example 2.6 to the decorated permutation of Example 2.10.

*Lemma 2.15.* [25, Lemma 16.2] The map  $\mathcal{I} \rightarrow \pi^\cdot(\mathcal{I})$  is a bijection from Grassmann necklaces  $\mathcal{I} = (I_1, \dots, I_n)$  of size  $n$  to decorated permutations  $\pi^\cdot(\mathcal{I})$  of size  $n$ . Under this bijection, the weak excedances of  $\pi^\cdot(\mathcal{I})$  are in positions  $I_1$ .

One particularly nice class of positroid cells is the *TP* or *totally positive* Schubert cells.

*Definition 2.16.* A *totally positive* Schubert cell is the intersection of a Schubert cell with  $(Gr_{k,n})_{\geq 0}$ .

TP Schubert cells are indexed by  $\mathbb{J}$ -diagrams such that all boxes are filled with a +.

<sup>1</sup>The convention of [25] was to place the boundary vertices in clockwise order.

<sup>2</sup>This forbidden pattern is in the shape of a backwards  $L$ , and hence is denoted  $\mathbb{J}$  and pronounced “Le.”

<sup>3</sup>Actually Postnikov’s convention was to set  $\pi^\cdot(i) = j$  above, so the decorated permutation we are associating is the inverse one to his.

### 3. A DEODHAR DECOMPOSITION OF THE GRASSMANNIAN

In this section we review Deodhar's decomposition of the flag variety  $G/B$  [8], and the parameterizations of the components due to Marsh and Rietsch [22]. We then give a Deodhar decomposition of the Grassmannian by projecting the usual Deodhar decomposition of the flag variety to the Grassmannian.

**3.1. The flag variety.** In this paper we fix the group  $G = \mathrm{SL}_n = \mathrm{SL}_n(\mathbb{R})$ , a maximal torus  $T$ , and opposite Borel subgroups  $B^+$  and  $B^-$ , which consist of the diagonal, upper-triangular, and lower-triangular matrices, respectively. We let  $U^+$  and  $U^-$  be the unipotent radicals of  $B^+$  and  $B^-$ ; these are the subgroups of upper-triangular and lower-triangular matrices with 1's on the diagonals. For each  $1 \leq i \leq n-1$  we have a homomorphism  $\phi_i : \mathrm{SL}_2 \rightarrow \mathrm{SL}_n$  such that

$$\phi_i \begin{pmatrix} a & b \\ c & d \end{pmatrix} = \begin{pmatrix} 1 & & & & & \\ & \ddots & & & & \\ & & a & b & & \\ & & c & d & & \\ & & & & \ddots & \\ & & & & & 1 \end{pmatrix} \in \mathrm{SL}_n,$$

that is,  $\phi_i$  replaces a  $2 \times 2$  block of the identity matrix with  $\begin{pmatrix} a & b \\ c & d \end{pmatrix}$ . Here  $a$  is at the  $(i+1)$ st diagonal entry counting from the southeast corner.<sup>4</sup> We use this to construct 1-parameter subgroups in  $G$  (landing in  $U^+$  and  $U^-$ , respectively) defined by

$$x_i(m) = \phi_i \begin{pmatrix} 1 & m \\ 0 & 1 \end{pmatrix} \quad \text{and} \quad y_i(m) = \phi_i \begin{pmatrix} 1 & 0 \\ m & 1 \end{pmatrix}, \quad \text{where } m \in \mathbb{R}.$$

Let  $W$  denote the Weyl group  $N_G(T)/T$ , where  $N_G(T)$  is the normalizer of  $T$ . The simple reflections  $s_i \in W$  are given explicitly by  $s_i := \dot{s}_i T$  where  $\dot{s}_i := \phi_i \begin{pmatrix} 0 & -1 \\ 1 & 0 \end{pmatrix}$  and any  $w \in W$  can be expressed as a product  $w = s_{i_1} s_{i_2} \dots s_{i_m}$  with  $m = \ell(w)$  factors. We set  $\dot{w} = \dot{s}_{i_1} \dot{s}_{i_2} \dots \dot{s}_{i_m}$ . For  $G = \mathrm{SL}_n$ , we have  $W = \mathfrak{S}_n$ , the symmetric group on  $n$  letters, and  $s_i$  is the transposition exchanging  $i$  and  $i+1$ .

We can identify the flag variety  $G/B$  with the variety  $\mathcal{B}$  of Borel subgroups, via

$$gB \longleftrightarrow g \cdot B^+ := gB^+g^{-1}.$$

We have two opposite Bruhat decompositions of  $\mathcal{B}$ :

$$\mathcal{B} = \bigsqcup_{w \in W} B^+ \dot{w} \cdot B^+ = \bigsqcup_{v \in W} B^- \dot{v} \cdot B^+.$$

We define the *Richardson variety*

$$\mathcal{R}_{v,w} := B^+ \dot{w} \cdot B^+ \cap B^- \dot{v} \cdot B^+,$$

the intersection of opposite Bruhat cells. This intersection is empty unless  $v \leq w$ , in which case it is smooth of dimension  $\ell(w) - \ell(v)$ , see [15, 21].

<sup>4</sup>Our numbering differs from that in [22] in that the rows of our matrices in  $\mathrm{SL}_n$  are numbered from the bottom.

**3.2. Distinguished expressions.** We now provide background on distinguished and positive distinguished subexpressions, as in [8] and [22]. We will assume that the reader is familiar with the (strong) Bruhat order  $<$  on the Weyl group  $W = \mathfrak{S}_n$ , and the basics of reduced expressions, as in [4].

Let  $\mathbf{w} := s_{i_1} \dots s_{i_m}$  be a reduced expression for  $w \in W$ . A *subexpression*  $\mathbf{v}$  of  $\mathbf{w}$  is a word obtained from the reduced expression  $\mathbf{w}$  by replacing some of the factors with 1. For example, consider a reduced expression in  $\mathfrak{S}_4$ , say  $s_3 s_2 s_1 s_3 s_2 s_3$ . Then  $s_3 s_2 1 s_3 s_2 1$  is a subexpression of  $s_3 s_2 s_1 s_3 s_2 s_3$ . Given a subexpression  $\mathbf{v}$ , we set  $v_{(k)}$  to be the product of the leftmost  $k$  factors of  $\mathbf{v}$ , if  $k \geq 1$ , and  $v_{(0)} = 1$ .

*Definition 3.1.* [22, 8] Given a subexpression  $\mathbf{v}$  of a reduced expression  $\mathbf{w} = s_{i_1} s_{i_2} \dots s_{i_m}$ , we define

$$\begin{aligned} J_{\mathbf{v}}^{\circ} &:= \{k \in \{1, \dots, m\} \mid v_{(k-1)} < v_{(k)}\}, \\ J_{\mathbf{v}}^{\square} &:= \{k \in \{1, \dots, m\} \mid v_{(k-1)} = v_{(k)}\}, \\ J_{\mathbf{v}}^{\bullet} &:= \{k \in \{1, \dots, m\} \mid v_{(k-1)} > v_{(k)}\}. \end{aligned}$$

The expression  $\mathbf{v}$  is called *non-decreasing* if  $v_{(j-1)} \leq v_{(j)}$  for all  $j = 1, \dots, m$ , e.g.  $J_{\mathbf{v}}^{\bullet} = \emptyset$ .

*Definition 3.2* (Distinguished subexpressions). [8, Definition 2.3] A subexpression  $\mathbf{v}$  of  $\mathbf{w}$  is called *distinguished* if we have

$$(3.1) \quad v_{(j)} \leq v_{(j-1)} s_{i_j} \quad \text{for all } j \in \{1, \dots, m\}.$$

In other words, if right multiplication by  $s_{i_j}$  decreases the length of  $v_{(j-1)}$ , then in a distinguished subexpression we must have  $v_{(j)} = v_{(j-1)} s_{i_j}$ .

We write  $\mathbf{v} < \mathbf{w}$  if  $\mathbf{v}$  is a distinguished subexpression of  $\mathbf{w}$ .

*Definition 3.3* (Positive distinguished subexpressions). We call a subexpression  $\mathbf{v}$  of  $\mathbf{w}$  a *positive distinguished subexpression* (or a PDS for short) if

$$(3.2) \quad v_{(j-1)} < v_{(j-1)} s_{i_j} \quad \text{for all } j \in \{1, \dots, m\}.$$

In other words, it is distinguished and non-decreasing.

*Lemma 3.4.* [22] Given  $v \leq w$  and a reduced expression  $\mathbf{w}$  for  $w$ , there is a unique PDS  $\mathbf{v}_+$  for  $v$  in  $\mathbf{w}$ .

**3.3. Deodhar components in the flag variety.** We now describe the Deodhar decomposition of the flag variety. This is a further refinement of the decomposition of  $G/B$  into Richardson varieties  $\mathcal{R}_{v,w}$ . Marsh and Rietsch [22] gave explicit parameterizations for each Deodhar component, identifying each one with a subset in the group.

*Definition 3.5.* [22, Definition 5.1] Let  $\mathbf{w} = s_{i_1} \dots s_{i_m}$  be a reduced expression for  $w$ , and let  $\mathbf{v}$  be a distinguished subexpression. Define a subset  $G_{\mathbf{v}, \mathbf{w}}$  in  $G$  by

$$(3.3) \quad G_{\mathbf{v}, \mathbf{w}} := \left\{ g = g_1 g_2 \dots g_m \left| \begin{array}{ll} g_{\ell} = x_{i_{\ell}}(m_{\ell}) \dot{s}_{i_{\ell}}^{-1} & \text{if } \ell \in J_{\mathbf{v}}^{\bullet}, \\ g_{\ell} = y_{i_{\ell}}(p_{\ell}) & \text{if } \ell \in J_{\mathbf{v}}^{\square}, \\ g_{\ell} = \dot{s}_{i_{\ell}} & \text{if } \ell \in J_{\mathbf{v}}^{\circ}, \end{array} \right. \text{ for } p_{\ell} \in \mathbb{R}^*, m_{\ell} \in \mathbb{R}. \right\}.$$

There is an obvious map  $(\mathbb{R}^*)^{|J_{\mathbf{v}}^{\square}|} \times \mathbb{R}^{|J_{\mathbf{v}}^{\bullet}|} \rightarrow G_{\mathbf{v}, \mathbf{w}}$  defined by the parameters  $p_{\ell}$  and  $m_{\ell}$  in (3.3). For  $v = w = 1$  we define  $G_{\mathbf{v}, \mathbf{w}} = \{1\}$ .

*Example 3.6.* Let  $W = \mathfrak{S}_5$ ,  $\mathbf{w} = s_2 s_3 s_4 s_1 s_2 s_3$  and  $\mathbf{v} = s_2 1 1 1 s_2 1$ . Then the corresponding element  $g \in G_{\mathbf{v}, \mathbf{w}}$  is given by  $g = s_2 y_3(p_2) y_4(p_3) y_1(p_4) x_2(m_5) s_2^{-1} y_3(p_6)$ , which is

$$g = \begin{pmatrix} 1 & 0 & 0 & 0 & 0 \\ p_3 & 1 & 0 & 0 & 0 \\ 0 & p_6 & 1 & 0 & 0 \\ p_2 p_3 & p_2 - m_5 p_6 & -m_5 & 1 & 0 \\ 0 & -p_4 p_6 & -p_4 & 0 & 1 \end{pmatrix}.$$

The following result from [22] gives an explicit parametrization for the Deodhar component  $\mathcal{R}_{\mathbf{v},\mathbf{w}}$ . We will take the description below as the *definition* of  $\mathcal{R}_{\mathbf{v},\mathbf{w}}$ .

*Proposition 3.7.* [22, Proposition 5.2] The map  $(\mathbb{R}^*)^{|\mathcal{J}_{\mathbf{v}}^{\square}|} \times \mathbb{R}^{|\mathcal{J}_{\mathbf{v}}^{\bullet}|} \rightarrow G_{\mathbf{v},\mathbf{w}}$  from Definition 3.5 is an isomorphism. The set  $G_{\mathbf{v},\mathbf{w}}$  lies in  $U^{-}\dot{v}\cap B^{+}\dot{w}B^{+}$ , and the assignment  $g \mapsto g \cdot B^{+}$  defines an isomorphism

$$(3.4) \quad G_{\mathbf{v},\mathbf{w}} \xrightarrow{\sim} \mathcal{R}_{\mathbf{v},\mathbf{w}}$$

between the subset  $G_{\mathbf{v},\mathbf{w}}$  of the group, and the Deodhar component  $\mathcal{R}_{\mathbf{v},\mathbf{w}}$  in the flag variety.

Suppose that for each  $w \in W$  we choose a reduced expression  $\mathbf{w}$  for  $w$ . Then it follows from Deodhar's work (see [8] and [22, Section 4.4]) that

$$(3.5) \quad \mathcal{R}_{v,w} = \bigsqcup_{\mathbf{v} \prec \mathbf{w}} \mathcal{R}_{\mathbf{v},\mathbf{w}} \quad \text{and} \quad G/B = \bigsqcup_{w \in W} \left( \bigsqcup_{\mathbf{v} \prec \mathbf{w}} \mathcal{R}_{\mathbf{v},\mathbf{w}} \right).$$

These are called the *Deodhar decompositions* of  $\mathcal{R}_{v,w}$  and  $G/B$ .

*Remark 3.8.* One may define the Richardson variety  $\mathcal{R}_{v,w}$  over a finite field  $\mathbb{F}_q$ . In this setting the number of points determine the  $R$ -polynomials  $R_{v,w}(q) = \#(\mathcal{R}_{v,w}(\mathbb{F}_q))$  introduced by Kazhdan and Lusztig [14] to give a formula for the Kazhdan-Lusztig polynomials. This was the original motivation for Deodhar's work. Therefore the isomorphisms  $\mathcal{R}_{\mathbf{v},\mathbf{w}} \cong (\mathbb{F}_q^*)^{|\mathcal{J}_{\mathbf{v}}^{\square}|} \times \mathbb{F}_q^{|\mathcal{J}_{\mathbf{v}}^{\bullet}|}$  together with the decomposition (3.5) give formulas for the  $R$ -polynomials.

**3.4. Projections of Deodhar components to the Grassmannian.** Now we consider the projection of the Deodhar decomposition to the Grassmannian  $Gr_{k,n}$ . Let  $W_k$  be the parabolic subgroup  $\langle s_1, s_2, \dots, \hat{s}_{n-k}, \dots, s_{n-1} \rangle$  of  $W = \mathfrak{S}_n$ , and let  $W^k$  denote the set of minimal-length coset representatives of  $W/W_k$ . Recall that a *descent* of a permutation  $\pi$  is a position  $j$  such that  $\pi(j) > \pi(j+1)$ . Then  $W^k$  is the subset of permutations of  $\mathfrak{S}_n$  which have at most one descent; and that descent must be in position  $n-k$ .

Let  $\pi_k : G/B \rightarrow Gr_{k,n}$  be the projection from the flag variety to the Grassmannian. For each  $w \in W^k$  and  $v \leq w$ , define  $\mathcal{P}_{v,w} = \pi_k(\mathcal{R}_{v,w})$ . Then by work of Lusztig [21],  $\pi_k$  is an isomorphism on  $\mathcal{P}_{v,w}$ , and we have a decomposition

$$(3.6) \quad Gr_{k,n} = \bigsqcup_{w \in W^k} \left( \bigsqcup_{v \leq w} \mathcal{P}_{v,w} \right).$$

*Definition 3.9.* For each reduced decomposition  $\mathbf{w}$  for  $w \in W^k$ , and each  $\mathbf{v} \prec \mathbf{w}$ , we define the (projected) *Deodhar component*  $\mathcal{P}_{\mathbf{v},\mathbf{w}} = \pi_k(\mathcal{R}_{\mathbf{v},\mathbf{w}}) \subset Gr_{k,n}$ .

*Lemma 3.10.* [20, Remark 3.12, Lemma 3.13] The decomposition in (3.6) coincides with the positroid stratification from Section 2.3. The appropriate bijection between the strata is defined as follows. Let  $\mathcal{Q}^k$  denote the set of pairs  $(v, w)$  where  $v \in W$ ,  $w \in W^k$ , and  $v \leq w$ ; let  $\text{Dec}_n^k$  denote the set of decorated permutations in  $S_n$  with  $k$  weak excedances. We consider both sets as partially ordered sets, where the cover relation corresponds to containment of closures of the corresponding strata. Then there is an order-preserving bijection  $\Phi$  from  $\mathcal{Q}^k$  to  $\text{Dec}_n^k$  which is defined as follows. Let  $(v, w) \in \mathcal{Q}^k$ . Then  $\Phi(v, w) = (\pi, \text{col})$  where  $\pi = vw^{-1}$ . We also let  $\pi^{\cdot}(v, w)$  denote  $\Phi(v, w)$ . To define  $\text{col}$ , we color any fixed point that occurs in one of the positions  $w(1), w(2), \dots, w(n-k)$  with the color  $-1$ , and color any other fixed point with the color  $1$ .

By Lemma 3.10,  $\mathcal{P}_{\mathbf{v},\mathbf{w}}$  lies in the positroid stratum  $S_{\pi^{\cdot}}$ . Note that the strata  $\mathcal{P}_{\mathbf{v},\mathbf{w}}$  do not depend on the chosen reduced decomposition of  $\mathbf{w}$  [19, Proposition 4.16].



Now if for each  $w \in W^k$  we choose a reduced decomposition  $\mathbf{w}$ , then we have

$$(3.7) \quad \mathcal{P}_{v,w} = \bigsqcup_{\mathbf{v} < \mathbf{w}} \mathcal{P}_{\mathbf{v},\mathbf{w}} \quad \text{and} \quad Gr_{k,n} = \bigsqcup_{w \in W^k} \left( \bigsqcup_{\mathbf{v} < \mathbf{w}} \mathcal{P}_{\mathbf{v},\mathbf{w}} \right).$$

Proposition 3.7 gives us a concrete way to think about the projected Deodhar components  $\mathcal{P}_{\mathbf{v},\mathbf{w}}$ . The projection  $\pi_k : G/B \rightarrow Gr_{k,n}$  maps each  $g \in G_{\mathbf{v},\mathbf{w}}$  to the span of its leftmost  $k$  columns:

$$g = \begin{pmatrix} g_{n,n} & \cdots & g_{n,n-k+1} & \cdots & g_{n,1} \\ \vdots & & \vdots & & \vdots \\ g_{1,n} & \cdots & g_{1,n-k+1} & \cdots & g_{1,1} \end{pmatrix} \mapsto A = \begin{pmatrix} g_{1,n-k+1} & \cdots & g_{n,n-k+1} \\ \vdots & & \vdots \\ g_{1,n} & \cdots & g_{n,n} \end{pmatrix}.$$

Alternatively, we may identify  $A \in Gr_{k,n}$  with its image in the Plücker embedding. Let  $e_i$  denote the column vector in  $\mathbb{R}^n$  such that the  $i$ th entry from the bottom contains a 1, and all other entries are 0, e.g.  $e_n = (1, 0, \dots, 0)^T$ , the transpose of the row vector  $(1, 0, \dots, 0)$ . Then the projection  $\pi_k$  maps each  $g \in G_{\mathbf{v},\mathbf{w}}$  (identified with  $g \cdot B^+ \in \mathcal{R}_{\mathbf{v},\mathbf{w}}$ ) to

$$(3.8) \quad g \cdot e_n \wedge \cdots \wedge e_{n-k+1} = \sum_{1 \leq j_1 < \cdots < j_k \leq n} \Delta_{j_1, \dots, j_k}(A) e_{j_k} \wedge \cdots \wedge e_{j_1}.$$

That is, the Plücker coordinate  $\Delta_{j_1, \dots, j_k}(A)$  is given by

$$\Delta_{j_1, \dots, j_k}(A) = \langle e_{j_k} \wedge \cdots \wedge e_{j_1}, g \cdot e_n \wedge \cdots \wedge e_{n-k+1} \rangle,$$

where  $\langle \cdot, \cdot \rangle$  is the usual inner product on  $\wedge^k \mathbb{R}^n$ .

*Example 3.11.* We continue Example 3.6. Note that  $w \in W^k$  where  $k = 2$ . Then the map  $\pi_2 : G_{\mathbf{v},\mathbf{w}} \rightarrow Gr_{2,5}$  is given by

$$g = \begin{pmatrix} 1 & 0 & 0 & 0 & 0 \\ p_3 & 1 & 0 & 0 & 0 \\ 0 & p_6 & 1 & 0 & 0 \\ p_2 p_3 & p_2 - m_5 p_6 & -m_5 & 1 & 0 \\ 0 & -p_4 p_6 & -p_4 & 0 & 1 \end{pmatrix} \longrightarrow A = \begin{pmatrix} -p_4 p_6 & p_2 - m_5 p_6 & p_6 & 1 & 0 \\ 0 & p_2 p_3 & 0 & p_3 & 1 \end{pmatrix}.$$

#### 4. DEODHAR COMPONENTS IN THE GRASSMANNIAN AND GO-DIAGRAMS

In this section we explain how to index the Deodhar components in the Grassmannian  $Gr_{k,n}$  by certain tableaux called *Go-diagrams*, which are fillings of Young diagrams by empty boxes,  $\bullet$ 's and  $\circ$ 's. We refer to the symbols  $\bullet$  and  $\circ$  as *black* and *white stones*. Recall that  $W_k = \langle s_1, s_2, \dots, \hat{s}_{n-k}, \dots, s_{n-1} \rangle$  is a parabolic subgroup of  $W = \mathfrak{S}_n$  and  $W^k$  is the set of minimal-length coset representatives of  $W/W_k$ .

We fix  $k$  and  $n$ , and let  $Q^k$  be the poset whose elements are the boxes in a  $k \times (n-k)$  rectangle. If  $b_1$  and  $b_2$  are two adjacent boxes such that  $b_2$  is immediately to the left or immediately above  $b_1$ , we have a cover relation  $b_1 < b_2$  in  $Q^k$ . The partial order on  $Q^k$  is the transitive closure of  $<$ . The middle and right diagram in the figure below show two linear extensions (or *reading orders*) of the poset  $Q^3$ , where  $n = 8$ . Next we assign a labeling of the boxes of  $Q^k$  by simple generators  $s_i$ , see the left diagram of the figure below. If  $b$  is a box labelled by  $s_i$ , we denote the simple generator labeling  $b$  by  $s_b := s_i$ .

The following result can be found in [29].

*Proposition 4.1.* Fix  $k$  and  $n$ . The upper order ideals of  $Q^k$  are in bijection with elements of  $W^k$ , and the different reading orders of  $Q^k$  allow us to compute all reduced expressions of elements of  $W^k$ . More specifically, let  $Y$  be an upper order ideal of  $Q^k$ , and choose a reading order  $e$  for the boxes of  $Y$ . Then if we read the labels of  $Y$  in the order specified by  $e$ , we will get a reduced word for some  $w \in W^k$ , and this element  $w$  does not depend on the choice of  $e$ . Therefore we may denote  $Y$  by  $O_w$ . Moreover, if we let  $e$  vary over all reading orders for boxes of  $Y$ , we will obtain all reduced expressions for  $w$ .

$s_5$	$s_4$	$s_3$	$s_2$	$s_1$
$s_6$	$s_5$	$s_4$	$s_3$	$s_2$
$s_7$	$s_6$	$s_5$	$s_4$	$s_3$

15	14	13	12	11
10	9	8	7	6
5	4	3	2	1

15	12	9	6	3
14	11	8	5	2
13	10	7	4	1

*Remark 4.2.* The upper order ideals of  $Q^k$  can be identified with the Young diagrams contained in a  $k \times (n - k)$  rectangle (justified at the upper left), and the reading orders of  $O_w$  can be identified with the *reverse* standard tableaux of shape  $O_w$ , i.e. entries decrease from left to right in rows and from top to bottom in columns.

**4.1. Go-diagrams and labeled Go-diagrams.** Next we will identify distinguished subexpressions of reduced words for elements of  $W^k$  with certain tableaux called *Go-diagrams*.

*Definition 4.3.* Let  $\mathbf{w}$  be a reduced expression for some  $w \in W^k$ , and consider a distinguished subexpression  $\mathbf{v}$  of  $\mathbf{w}$ . Let  $O_w$  be the Young diagram associated to  $w$  and choose the reading order of its boxes which corresponds to  $\mathbf{w}$ . Then for each  $k \in J_{\mathbf{v}}^{\circ}$  we will place a  $\circ$  in the corresponding box of  $O_w$ ; for each  $k \in J_{\mathbf{v}}^{\bullet}$  we will place a  $\bullet$  in the corresponding box; and for each  $k \in J_{\mathbf{v}}^{\square}$  we will leave the corresponding box blank. We call the resulting diagram a *Go-diagram*, and refer to the symbols  $\circ$  and  $\bullet$  as *white* and *black stones*.

*Remark 4.4.* Note that a Go-diagram has no black stones if and only if  $\mathbf{v}$  is a positive distinguished subexpression of  $\mathbf{w}$ . In this case, if we replace the empty boxes by  $+$ 's and the white stones by  $0$ 's, we will get a  $\mathbb{J}$ -diagram. Therefore, slightly abusing terminology, we will often refer to a Go-diagram with no black stones as a  $\mathbb{J}$ -diagram.<sup>5</sup> Moreover, the Go-diagrams with no black stones are in bijection with  $\mathbb{J}$ -diagrams. See [20, Section 4] for more details.

*Example 4.5.* Consider the upper order ideal  $O_w$  which is  $Q^k$  itself for  $\mathfrak{S}_5$  and  $k = 2$ . Then  $Q^k$  is the poset shown in the left diagram. Let us choose the reading order indicated by the labeling shown in the right diagram.

$s_3$	$s_2$	$s_1$
$s_4$	$s_3$	$s_2$

6	5	4
3	2	1

Now consider the distinguished subexpressions  $s_2s_3s_4s_1s_2s_3$ ,  $1s_3s_4s_11s_3$ , and  $1s_31s_11s_3$  of the reduced expression  $\mathbf{w} = s_2s_3s_4s_1s_2s_3$  corresponding to our chosen reading order. Among these three subexpressions, the first and second are PDS's. The corresponding Go-diagrams are as follows.

$\circ$	$\circ$	$\circ$
$\circ$	$\circ$	$\circ$

$\circ$		$\circ$
$\circ$	$\circ$	

$\bullet$		$\circ$
	$\circ$	

The reader might worry that Definition 4.3 has too much dependence on the choice of reduced expression  $\mathbf{w}$ , or equivalently on the reading order  $e$ . However, we have the following result.

*Proposition 4.6.* [20, Proposition 4.5] Let  $D$  be a Go-diagram in a Young diagram  $O_w$ . Choose any reading order  $e$  for the boxes of  $O_w$ . Let  $\mathbf{w}$  be the corresponding reduced expression for  $w$ . Let  $\mathbf{v}(D)$

<sup>5</sup>Since  $\mathbb{J}$ -diagrams are a special case of Go-diagrams, one might also refer to them as *Lego* diagrams.

be the subexpression of  $\mathbf{w}$  obtained as follows: if a box  $b$  of  $D$  contains a black or white stone then the corresponding simple generator  $s_b$  is present in the subexpression, while if  $b$  is empty, we omit the corresponding simple generator. Then we have the following:

- (1) the element  $v := v(D)$  is independent of the choice of reading word  $e$ .
- (2) whether  $\mathbf{v}(D)$  is a PDS depends only on  $D$  (and not  $e$ ).
- (3) whether  $\mathbf{v}(D)$  is distinguished depends only on  $D$  (and not on  $e$ ).

*Definition 4.7.* Let  $O_w$  be an upper order ideal of  $Q^k$ , where  $w \in W^k$  and  $W = S_n$ . Consider a Go-diagram  $D$  of shape  $O_w$ ; this is contained in a  $k \times (n - k)$  rectangle, and the shape  $O_w$  gives rise to a lattice path from the northeast corner to the southwest corner of the rectangle. Label the steps of that lattice path from 1 to  $n$ ; this gives a natural labeling to every row and column of the rectangle. We now let  $v := v(D)$ , and we define  $\pi^\cdot(D)$  to be the decorated permutation  $(\pi(D), \text{col})$  where  $\pi = \pi(D) = vw^{-1}$ . The fixed points of  $\pi$  correspond precisely to rows and columns of the rectangle with no  $+$ 's. If there are no  $+$ 's in the row (respectively, column) labeled by  $h$ , then  $\pi(h) = h$  and this fixed point gets colored with color 1 (respectively,  $-1$ ).

*Remark 4.8.* It follows from Lemma 3.10 that the projected Deodhar component  $\mathcal{P}_D$  corresponding to  $D$  is contained in the positroid stratum  $S_{\pi^\cdot(D)}$ .

*Remark 4.9.* Recall from Remark 3.8 that the isomorphisms  $\mathcal{R}_{\mathbf{v}, \mathbf{w}} \cong (\mathbb{F}_q^*)^{|J_\square^\square|} \times \mathbb{F}_q^{|J_\square^\bullet|}$  together with the decomposition (3.5) give formulas for the  $R$ -polynomials. Therefore a good characterization of Go-diagrams could lead to explicit formulas for the corresponding  $R$ -polynomials.

If we choose a reading order of  $O_w$ , then we will also associate to a Go-diagram of shape  $O_w$  a *labeled Go-diagram*, as defined below. Equivalently, a labeled Go-diagram is associated to a pair  $(\mathbf{v}, \mathbf{w})$ .

*Definition 4.10.* Given a reading order of  $O_w$  and a Go-diagram of shape  $O_w$ , we obtain a *labeled Go-diagram* by replacing each  $\circ$  with a 1, each  $\bullet$  with a  $-1$ , and putting a  $p_i$  in each blank square  $b$ , where the subscript  $i$  corresponds to the label of  $b$  inherited from the reading order.

The labeled Go-diagrams corresponding to the Go-diagrams from Example 4.5 are:

$$\begin{array}{|c|c|c|} \hline 1 & 1 & 1 \\ \hline 1 & 1 & 1 \\ \hline \end{array}
 \qquad
 \begin{array}{|c|c|c|} \hline 1 & p_5 & 1 \\ \hline 1 & 1 & p_1 \\ \hline \end{array}
 \qquad
 \begin{array}{|c|c|c|} \hline -1 & p_5 & 1 \\ \hline p_3 & 1 & p_1 \\ \hline \end{array}$$

**4.2. Plücker coordinates for projected Deodhar components.** Consider  $\mathcal{P}_{\mathbf{v}, \mathbf{w}} \subset Gr_{k, n}$ , where  $\mathbf{w}$  is a reduced expression for  $w \in W^k$  and  $\mathbf{v} \prec \mathbf{w}$ . Here we provide some formulas for the Plücker coordinates of the elements of  $\mathcal{P}_{\mathbf{v}, \mathbf{w}}$ , in terms of the parameters used to define  $G_{\mathbf{v}, \mathbf{w}}$ . Some of these formulas are related to corresponding formulas for  $G/B$  in [22, Section 7].

*Theorem 4.11.* [20, Lemma 5.1, Theorem 5.2] Choose any element  $A$  of  $\mathcal{P}_{\mathbf{v}, \mathbf{w}} \subset Gr_{k, n}$ , in other words,  $A = \pi_k(g)$  for some  $g \in G_{\mathbf{v}, \mathbf{w}}$ . Then the lexicographically minimal and maximal nonzero Plücker coordinates of  $A$  are  $\Delta_I$  and  $\Delta_{I'}$ , where

$$I = w \{n, n - 1, \dots, n - k + 1\} \quad \text{and} \quad I' = v \{n, n - 1, \dots, n - k + 1\}.$$

Moreover, if we write  $g = g_1 \dots g_m$  as in Definition 3.5, then

$$(4.1) \quad \Delta_I(A) = (-1)^{|J_\square^\bullet|} \prod_{i \in J_\square^\square} p_i \quad \text{and} \quad \Delta_{I'}(A) = 1.$$

Note that  $\Delta_I(A)$  equals the product of all the labels from the labeled Go-diagram associated to  $(\mathbf{v}, \mathbf{w})$ .

This theorem can be extended to provide a formula for some other Plücker coordinates. Let  $b$  be any box of  $D$ . We can choose a linear extension  $e$  of the boxes of  $D$  which orders the boxes which are weakly southeast of  $b$  (the *inner boxes*) before the rest (the *outer boxes*). This gives rise to a reduced expression  $\mathbf{w}$  and subexpression  $\mathbf{v}$ , as well as reduced expressions  $\mathbf{w}_b^{\text{in}} = \mathbf{w}^{\text{in}}$ ,  $\mathbf{v}_b^{\text{in}} = \mathbf{v}^{\text{in}}$ ,  $\mathbf{w}_b^{\text{out}} = \mathbf{w}^{\text{out}}$ , and  $\mathbf{v}_b^{\text{out}} = \mathbf{v}^{\text{out}}$ , which are obtained by restricting  $\mathbf{w}$  and  $\mathbf{v}$  to the inner and outer boxes, respectively.

*Theorem 4.12.* [20, Theorem 5.6] Let  $\mathbf{w} = s_{i_1} \dots s_{i_m}$  be a reduced expression for  $w \in W^k$  and  $\mathbf{v} \prec \mathbf{w}$ , and let  $D$  be the corresponding Go-diagram. Choose any box  $b$  of  $D$ , and let  $v^{\text{in}} = v_b^{\text{in}}$  and  $w^{\text{in}} = w_b^{\text{in}}$ , and  $v^{\text{out}} = v_b^{\text{out}}$  and  $w^{\text{out}} = w_b^{\text{out}}$ . Let  $A = \pi_k(g)$  for any  $g \in G_{\mathbf{v}, \mathbf{w}}$ , and let  $I = w\{n, n-1, \dots, n-k+1\}$ . Define  $I_b = v^{\text{in}}(w^{\text{in}})^{-1}I \in \binom{[n]}{k}$ . If we write  $g = g_1 \dots g_m$  as in Definition 3.5, then

$$(4.2) \quad \Delta_{I_b}(A) = (-1)^{|J_{\mathbf{v}^{\text{out}}}^{\bullet}|} \prod_{i \in J_{\mathbf{v}^{\text{out}}}^{\square}} p_i.$$

Note that  $\Delta_{I_b}(A)$  equals the product of all the labels in the “out” boxes of the labeled Go-diagram.

*Example 4.13.* Consider  $A \in Gr_{3,7}$  which is the projection of  $g \in G_{\mathbf{v}, \mathbf{w}}$  with

$$\mathbf{w} = s_3 s_4 s_5 s_6 s_2 s_3 s_4 s_5 s_1 s_2 s_3 s_4, \quad \mathbf{v} = s_3 1 s_5 1 s_2 s_3 1 s_5 1 s_2 s_3 s_4.$$

Then  $v = s_2 s_4$  and  $\pi = vv^{-1} = (4, 6, 7, 1, 3, 2, 5)$ . The Go-diagram and the labeled Go-diagram are as follows:

○	●	●	
●		○	○
	○		○

1	-1	-1	$p_9$
-1	$p_7$	1	1
$p_4$	1	$p_2$	1

467	456	245	234
167	156	125	123
127	125	125	123

Each box  $b$  in the diagram on the right show the subset  $I_b$ . Then we have

$$\begin{aligned} \Delta_{1,2,3} &= -p_2 p_4 p_7 p_9, & \Delta_{1,2,5} &= -p_4 p_7 p_9, & \Delta_{1,2,7} &= -p_7 p_9, & \Delta_{1,5,6} &= -p_4 p_9, \\ \Delta_{1,6,7} &= p_9, & \Delta_{2,3,4} &= -p_2 p_4 p_7, & \Delta_{2,4,5} &= p_4 p_7, & \Delta_{4,5,6} &= -p_4, & \Delta_{4,6,7} &= 1. \end{aligned}$$

## 5. SOLITON SOLUTIONS TO THE KP EQUATION AND THEIR CONTOUR PLOTS

We now explain how to obtain a soliton solution to the KP equation from a point of  $Gr_{k,n}$ .

**5.1. From a point of the Grassmannian to a  $\tau$ -function.** We start by fixing real parameters  $\kappa_i$  such that  $\kappa_1 < \kappa_2 < \dots < \kappa_n$ , which are *generic*, in the sense that the sums  $\sum_{j=1}^p \kappa_{i_j}$  are all distinct for any  $p$  with  $1 < p < n$ . We also assume that the differences between consecutive  $\kappa_i$ 's are similar, that is,  $\kappa_{i+1} - \kappa_i$  is of order one.

Let  $\{E_i; i = 1, \dots, m\}$  be a set of exponential functions in  $(x, y, t) \in \mathbb{R}^3$  defined by

$$E_i(x, y, t) := \exp \theta_i(x, y, t) \quad \text{where} \quad \theta_i(x, y, t) = \kappa_i x + \kappa_i^2 y + \kappa_i^3 t.$$

Thinking of each  $E_i$  as a function of  $x$ , we see that the elements  $\{E_i\}$  are linearly independent, because their Wronskian determinant with respect to  $x$  is non zero:

$$\text{Wr}(E_1, \dots, E_n) := \det[(E_i^{(j-1)})_{1 \leq i, j \leq n}] = \prod_{i < j} (\kappa_j - \kappa_i) E_1 \cdots E_n \neq 0.$$

Here  $E_i^{(j)} := \partial^j E_i / \partial x^j = \kappa_i^j E_i$ .

Let  $A$  be a full rank  $k \times n$  matrix. We define a set of functions  $\{f_1, \dots, f_k\}$  by

$$(f_1, f_2, \dots, f_k)^T = A \cdot (E_1, E_2, \dots, E_n)^T,$$

where  $(\dots)^T$  denotes the transpose of the vector  $(\dots)$ .

Since the exponential functions  $\{E_i\}$  are linearly independent, we identify them as a basis of  $\mathbb{R}^n$ , and then  $\{f_1, \dots, f_k\}$  spans a  $k$ -dimensional subspace. This identification can be seen, more precisely, as  $E_i \leftrightarrow (1, \kappa_i, \dots, \kappa_i^{n-1})^T \in \mathbb{R}^n$ . This subspace depends only on which point of the Grassmannian  $Gr_{k,n}$  the matrix  $A$  represents, so we can identify the space of subspaces  $\{f_1, \dots, f_k\}$  with  $Gr_{k,n}$ .

The  $\tau$ -function of  $A$  is defined by

$$(5.1) \quad \tau_A(x, y, t) := \text{Wr}(f_1, f_2, \dots, f_k).$$

For  $I = \{i_1, \dots, i_k\} \in \binom{[n]}{k}$ , we set

$$E_I(x, y, t) := \text{Wr}(E_{i_1}, E_{i_2}, \dots, E_{i_k}) = \prod_{\ell < m} (\kappa_{i_m} - \kappa_{i_\ell}) E_{i_1} \cdots E_{i_k} > 0.$$

Applying the Binet-Cauchy identity to the fact that  $f_j = \sum_{i=1}^n a_{ji} E_i$ , we get

$$(5.2) \quad \tau_A(x, y, t) = \sum_{I \in \binom{[n]}{k}} \Delta_I(A) E_I(x, y, t).$$

It follows that if  $A \in (Gr_{k,n})_{\geq 0}$ , then  $\tau_A > 0$  for all  $(x, y, t) \in \mathbb{R}^3$ .

Thinking of  $\tau_A$  as a function of  $A$ , we note from (5.2) that the  $\tau$ -function encodes the information of the Plücker embedding. More specifically, if we identify each function  $E_I$  with  $I = \{i_1, \dots, i_k\}$  with the wedge product  $E_{i_1} \wedge \cdots \wedge E_{i_k}$  (recall the identification  $E_i \leftrightarrow (1, \kappa_i, \dots, \kappa_i^{n-1})^T$ ), then the map  $\tau : Gr_{k,n} \hookrightarrow \mathbb{RP}^{\binom{n}{k}-1}$ ,  $A \mapsto \tau_A$  has the Plücker coordinates as coefficients.

**5.2. From the  $\tau$ -function to solutions of the KP equation.** The KP equation for  $u(x, y, t)$

$$\frac{\partial}{\partial x} \left( -4 \frac{\partial u}{\partial t} + 6u \frac{\partial u}{\partial x} + \frac{\partial^3 u}{\partial x^3} \right) + 3 \frac{\partial^2 u}{\partial y^2} = 0$$

was proposed by Kadomtsev and Petviashvili in 1970 [13], in order to study the stability of the soliton solutions of the Korteweg-de Vries (KdV) equation under the influence of weak transverse perturbations. The KP equation can be also used to describe two-dimensional shallow water wave phenomena (see for example [17]). This equation is now considered to be a prototype of an integrable nonlinear partial differential equation. For more background, see [24, 9, 1, 12, 23].

It is well known (see [12, 5, 6, 7]) that the  $\tau$ -function defined in (5.1) provides a soliton solution of the KP equation,

$$(5.3) \quad u_A(x, y, t) = 2 \frac{\partial^2}{\partial x^2} \ln \tau_A(x, y, t).$$

It is easy to show that if  $A \in (Gr_{k,n})_{\geq 0}$ , then such a solution  $u_A(x, y, t)$  is regular for all  $(x, y, t) \in \mathbb{R}^3$ . For this reason we are interested in solutions  $u_A(x, y, t)$  of the KP equation which come from points  $A$  of  $(Gr_{k,n})_{\geq 0}$ . Throughout this paper when we speak of a *soliton solution to the KP equation*, we will mean a solution  $u_A(x, y, t)$  which has form (5.3).

**5.3. Contour plots of soliton solutions.** One can visualize a solution  $u_A(x, y, t)$  to the KP equation by drawing level sets of the solution in the  $xy$ -plane, when the coordinate  $t$  is fixed. For each  $r \in \mathbb{R}$ , we denote the corresponding level set by

$$C_r(t) := \{(x, y) \in \mathbb{R}^2 : u_A(x, y, t) = r\}.$$

Figure 2 depicts both a three-dimensional image of a solution  $u_A(x, y, t)$ , as well as multiple level sets  $C_r$ . These level sets are lines parallel to the line of the wave peak.

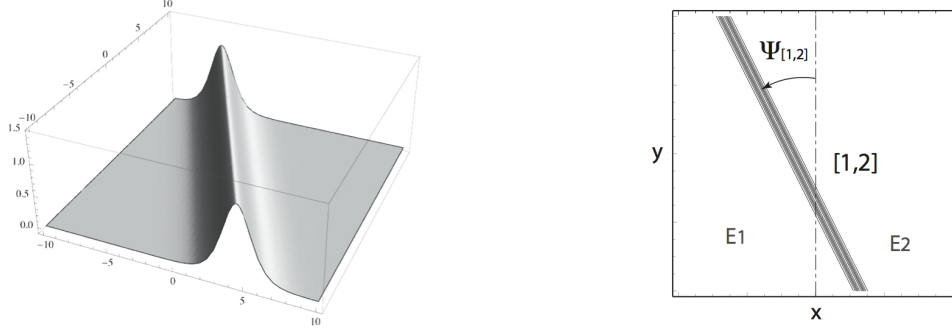


FIGURE 2. A line-soliton solution  $u_A(x, y, t)$  where  $A = (1, 1) \in (Gr_{1,2})_{\geq 0}$ , depicted via the 3-dimensional profile  $u_A(x, y, t)$ , and the level sets of  $u_A(x, y, t)$  for some  $t$ .  $E_i$  represents the dominant exponential in each region.

To study the behavior of  $u_A(x, y, t)$  for  $A \in S_{\mathcal{M}} \subset Gr_{k,n}$ , we consider the dominant exponentials in the  $\tau$ -function (5.2) at each point  $(x, y, t)$ . First we write the  $\tau$ -function in the form

$$\begin{aligned} \tau_A(x, y, t) &= \sum_{J \in \binom{[n]}{k}} \Delta_J(A) E_J(x, y, t) \\ &= \sum_{J \in \mathcal{M}} \exp \left( \sum_{i=1}^n (\kappa_{j_i} x + \kappa_{j_i}^2 y + \kappa_{j_i}^3 t) + \ln(\Delta_J(A) K_J) \right), \end{aligned}$$

where  $K_J := \prod_{\ell < m} (\kappa_{j_m} - \kappa_{j_\ell}) > 0$ . Note that in general the terms  $\ln(\Delta_J(A) K_J)$  could be imaginary when some  $\Delta_J(A)$  are negative.

Since we are interested in the behavior of the soliton solutions when the variables  $(x, y, t)$  are on a large scale, we rescale the variables with a small positive number  $\epsilon$ ,

$$x \longrightarrow \frac{x}{\epsilon}, \quad y \longrightarrow \frac{y}{\epsilon}, \quad t \longrightarrow \frac{t}{\epsilon}.$$

This leads to

$$\tau_A^\epsilon(x, y, t) = \sum_{J \in \mathcal{M}} \exp \left( \frac{1}{\epsilon} \sum_{i=1}^n (\kappa_{j_i} x + \kappa_{j_i}^2 y + \kappa_{j_i}^3 t) + \ln(\Delta_J(A) K_J) \right).$$

Then we define a function  $f_A(x, y, t)$  as the limit

$$\begin{aligned} f_A(x, y, t) &= \lim_{\epsilon \rightarrow 0} \epsilon \ln(\tau_A^\epsilon(x, y, t)) \\ (5.4) \quad &= \max_{J \in \mathcal{M}} \left\{ \sum_{i=1}^k (\kappa_{j_i} x + \kappa_{j_i}^2 y + \kappa_{j_i}^3 t) \right\}. \end{aligned}$$

Since the above function depends only on the collection  $\mathcal{M}$ , we also denote it as  $f_{\mathcal{M}}(x, y, t)$ .

*Definition 5.1.* Given a solution  $u_A(x, y, t)$  of the KP equation as in (5.3), we define its *contour plot*  $\mathcal{C}(u_A)$  to be the locus in  $\mathbb{R}^3$  where  $f_A(x, y, t)$  is not linear. If we fix  $t = t_0$ , then we let  $\mathcal{C}_{t_0}(u_A)$  be the locus in  $\mathbb{R}^2$  where  $f_A(x, y, t = t_0)$  is not linear, and we also refer to this as a *contour plot*. Because these contour plots depend only on  $\mathcal{M}$  and not on  $A$ , we also refer to them as  $\mathcal{C}(\mathcal{M})$  and  $\mathcal{C}_{t_0}(\mathcal{M})$ .

*Remark 5.2.* The contour plot approximates the locus where  $|u_A(x, y, t)|$  takes on its maximum values or is singular.

*Remark 5.3.* Note that the contour plot generated by the function  $f_A(x, y, t)$  at  $t = 0$  consists of a set of semi-infinite lines attached to the origin  $(0, 0)$  in the  $xy$ -plane. And if  $t_1$  and  $t_2$  have the same sign, then the corresponding contour plots  $\mathcal{C}_{t_1}(\mathcal{M})$  and  $\mathcal{C}_{t_2}(\mathcal{M})$  are self-similar.

Also note that because our definition of the contour plot ignores the constant terms  $\ln(\Delta_J(A)K_J)$ , there are no phase-shifts in our picture, and the contour plot for  $f_A(x, y, t) = f_{\mathcal{M}}(x, y, t)$  does not depend on the signs of the Plücker coordinates.

It follows from Definition 5.1 that  $\mathcal{C}(u_A)$  and  $\mathcal{C}_{t_0}(u_A)$  are piecewise linear subsets of  $\mathbb{R}^3$  and  $\mathbb{R}^2$ , respectively, of codimension 1. In fact it is easy to verify the following.

*Proposition 5.4.* [19, Proposition 4.3] If each  $\kappa_i$  is an integer, then  $\mathcal{C}(u_A)$  is a tropical hypersurface in  $\mathbb{R}^3$ , and  $\mathcal{C}_{t_0}(u_A)$  is a tropical hypersurface (i.e. a tropical curve) in  $\mathbb{R}^2$ .

The contour plot  $\mathcal{C}_{t_0}(u_A)$  consists of line segments called *line-solitons*, some of which have finite length, while others are unbounded and extend in the  $y$  direction to  $\pm\infty$ . Each region of the complement of  $\mathcal{C}_{t_0}(u_A)$  in  $\mathbb{R}^2$  is a domain of linearity for  $f_A(x, y, t)$ , and hence each region is naturally associated to a *dominant exponential*  $\Delta_J(A)E_J(x, y, t)$  from the  $\tau$ -function (5.2). We label this region by  $J$  or  $E_J$ . Each line-soliton represents a balance between two dominant exponentials in the  $\tau$ -function.

Because of the genericity of the  $\kappa$ -parameters, the following lemma is immediate.

*Lemma 5.5.* [7, Proposition 5] The index sets of the dominant exponentials of the  $\tau$ -function in adjacent regions of the contour plot in the  $xy$ -plane are of the form  $\{i, l_2, \dots, l_k\}$  and  $\{j, l_2, \dots, l_k\}$ .

We call the line-soliton separating the two dominant exponentials in Lemma 5.5 a *line-soliton of type*  $[i, j]$ . Its equation is

$$(5.5) \quad x + (\kappa_i + \kappa_j)y + (\kappa_i^2 + \kappa_i\kappa_j + \kappa_j^2)t = 0.$$

*Remark 5.6.* Consider a line-soliton given by (5.5). Compute the angle  $\Psi_{[i, j]}$  between the positive  $y$ -axis and the line-soliton of type  $[i, j]$ , measured in the counterclockwise direction, so that the negative  $x$ -axis has an angle of  $\frac{\pi}{2}$  and the positive  $x$ -axis has an angle of  $-\frac{\pi}{2}$ . Then  $\tan \Psi_{[i, j]} = \kappa_i + \kappa_j$ , so we refer to  $\kappa_i + \kappa_j$  as the *slope* of the  $[i, j]$  line-soliton (see Figure 2).

In Section 7 we will explore the combinatorial structure of contour plots, that is, the ways in which line-solitons may interact. Generically we expect a point at which several line-solitons meet to have degree 3; we regard such a point as a trivalent vertex. Three line-solitons meeting at a trivalent vertex exhibit a *resonant interaction* (this corresponds to the *balancing condition* for a tropical curve). See [19, Section 4.2]. One may also have two line-solitons which cross over each other, forming an  $X$ -shape: we call this an  *$X$ -crossing*, but do not regard it as a vertex. See Figure 4. Vertices of degree greater than 4 are also possible.

*Definition 5.7.* Let  $i < j < k < \ell$  be positive integers. An  $X$ -crossing involving two line-solitons of types  $[i, k]$  and  $[j, \ell]$  is called a *black  $X$ -crossing*. An  $X$ -crossing involving two line-solitons of types  $[i, j]$  and  $[k, \ell]$ , or of types  $[i, \ell]$  and  $[j, k]$ , is called a *white  $X$ -crossing*.

*Definition 5.8.* A contour plot  $\mathcal{C}_t(u_A)$  is called *generic* if all interactions of line-solitons are at trivalent vertices or are  $X$ -crossings.

## 6. UNBOUNDED LINE-SOLITONS AT $y \gg 0$ AND $y \ll 0$

In this section we explain that the unbounded line-solitons at  $|y| \gg 0$  of a contour plot  $\mathcal{C}_t(u_A)$  are determined by which positroid stratum contains  $A$ . Conversely, the unbounded line-solitons of  $\mathcal{C}_t(u_A)$  determine which positroid stratum  $A$  lies in.

*Theorem 6.1.* [20, Theorem 8.1] Let  $A \in Gr_{k, n}$  lie in the positroid stratum  $S_{\pi^\cdot}$ , where  $\pi^\cdot = (\pi, col)$ . Consider the contour plot  $\mathcal{C}_t(u_A)$  for any time  $t$ . Then the excedances (respectively, nonexcedances) of  $\pi$  are in bijection with the unbounded line-solitons of  $\mathcal{C}_t(u_A)$  at  $y \gg 0$  (respectively,  $y \ll 0$ ). More specifically, in  $\mathcal{C}_t(u_A)$ ,

- (a) there is an unbounded line-soliton of  $[i, h]$ -type at  $y \gg 0$  if and only if  $\pi(i) = h$  for  $i < h$ ,
- (b) there is an unbounded line-soliton of  $[i, h]$ -type at  $y \ll 0$  if and only if  $\pi(h) = i$  for  $i < h$ .

Therefore  $\pi$  determines the unbounded line-solitons at  $y \gg 0$  and  $y \ll 0$  of  $\mathcal{C}_t(u_A)$  for any time  $t$ .

Conversely, given a contour plot  $\mathcal{C}_t(u_A)$  at any time  $t$  where  $A \in Gr_{k,n}$ , one can construct  $\pi = (\pi, col)$  such that  $A \in S_\pi$  as follows. The excedances and nonexcedances of  $\pi$  are constructed as above from the unbounded line-solitons. If there is an  $h \in [n]$  such that  $h \in J$  for every dominant exponential  $E_J$  labeling the contour plot, then set  $\pi(h) = h$  with  $col(h) = 1$ . If there is an  $h \in [n]$  such that  $h \notin J$  for any dominant exponential  $E_J$  labeling the contour plot, then set  $\pi(h) = h$  with  $col(h) = -1$ .

*Remark 6.2.* Chakravarty and Kodama [5, Prop. 2.6 and 2.9] and [7, Theorem 5] associated a derangement to each *irreducible* element  $A$  in the *totally non-negative part*  $(Gr_{k,n})_{\geq 0}$  of the Grassmannian. Theorem 6.1 generalizes their result by dropping the hypothesis of irreducibility and extending the setting from  $(Gr_{k,n})_{\geq 0}$  to  $Gr_{k,n}$ .

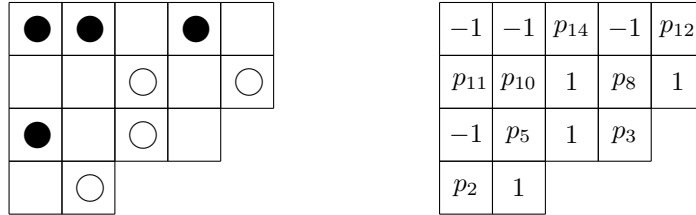
*Example 6.3.* Consider some  $A \in Gr_{4,9}$  which is the projection of an element  $g \in G_{\mathbf{v}, \mathbf{w}}$  with

$$\mathbf{w} = s_7 s_8 s_4 s_5 s_6 s_7 s_2 s_4 s_5 s_6 s_1 s_2 s_3 s_4 s_5 \quad \text{and} \quad \mathbf{v} = s_7 1 1 s_5 1 s_7 s_2 1 s_4 1 1 1 s_2 1 s_4 s_5.$$

Then  $v = 1$  and  $\pi = vw^{-1} = (6, 7, 1, 8, 2, 3, 9, 4, 5)$ . The matrix  $g \in G_{\mathbf{v}, \mathbf{w}}$  is given by

$$g = \dot{s}_7 y_8(p_2) y_4(p_3) \dot{s}_5 y_6(p_5) x_7(m_6) \dot{s}_7^{-1} \dot{s}_2 y_3(p_8) \dot{s}_4 y_5(p_{10}) y_6(p_{11}) \\ \cdot y_1(p_{12}) x_2(m_{13}) \dot{s}_2^{-1} y_3(p_{14}) x_4(m_{15}) \dot{s}_4^{-1} x_5(m_{16}) \dot{s}_5^{-1}.$$

The Go-diagram and the labeled Go-diagram are as follows:



The  $A$ -matrix is then given by

$$A = \begin{pmatrix} -p_{12}p_{14} & q_{13} & p_{14} & q_{15} & -m_{16} & 1 & 0 & 0 & 0 \\ 0 & p_8 p_{10} p_{11} & 0 & p_{11}(p_3 + p_{10}) & p_{11} & 0 & 1 & 0 & 0 \\ 0 & 0 & 0 & -p_3 p_5 & -p_5 & 0 & -m_6 & 1 & 0 \\ 0 & 0 & 0 & 0 & 0 & 0 & p_2 & 0 & 1 \end{pmatrix},$$

where the matrix entry  $q_{13} = -m_{13}p_{14} + m_{15}p_8 - m_{16}p_8p_{10}$  and  $q_{15} = m_{15} - m_{16}(p_3 + p_{10})$ . In Figure 3, we show contour plots  $\mathcal{C}_t(u_A)$  for the solution  $u_A(x, y, t)$  at  $t = -10, 0, 10$ , using the choice of parameters  $(\kappa_1, \dots, \kappa_9) = (-5, -3, -2, -1, 0, 1, 2, 3, 4)$ ,  $p_j = 1$  for all  $j$ , and  $m_\ell = 0$  for all  $\ell$ . Note that:

- (a) For  $y \gg 0$ , there are four unbounded line-solitons, whose types from right to left are:

$$[1, 6], \quad [2, 7], \quad [4, 8], \quad \text{and} \quad [7, 9]$$

- (b) For  $y \ll 0$ , there are five unbounded line-solitons, whose types from left to right are:

$$[1, 3], \quad [2, 5], \quad [3, 6], \quad [4, 8], \quad \text{and} \quad [5, 9]$$

We can see from this example that the line-solitons for  $y \gg 0$  correspond to the excedances in  $\pi = (6, 7, 1, 8, 2, 3, 9, 4, 5)$ , while those for  $y \ll 0$  correspond to the nonexcedances.

Note that if there are two adjacent regions of the contour plot whose Plücker coordinates have different signs, then the line-soliton separating them is singular. For example, the line-soliton of type  $[4, 8]$  (the



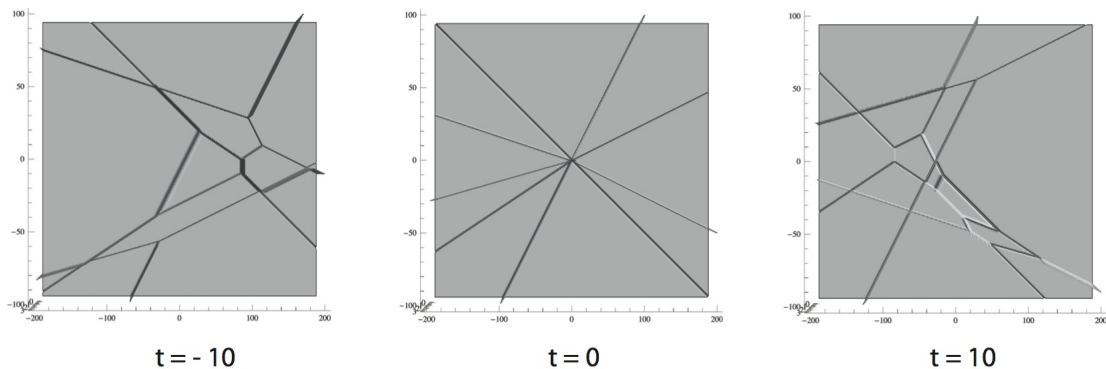


FIGURE 3. Example of contour plots  $\mathcal{C}_t(u_A)$  for  $A \in Gr_{4,9}$ . The contour plots are obtained by “Plot3D” of Mathematica (see the details in the text).

second soliton from the left in  $y \gg 0$ ) is singular, because the Plücker coordinates corresponding to the (dominant exponentials of the) adjacent regions are

$$\Delta_{1,2,4,9} = p_3 p_5 p_8 p_{10} p_{11} p_{12} p_{14} = 1 \quad \text{and} \quad \Delta_{1,2,8,9} = -p_8 p_{10} p_{11} p_{12} p_{14} = -1.$$

## 7. SOLITON GRAPHS AND GENERALIZED PLABIC GRAPHS

The following notion of *soliton graph* forgets the metric data of the contour plot, but preserves the data of how line-solitons interact and which exponentials dominate.

*Definition 7.1.* Let  $A \in Gr_{k,n}$  and consider a generic contour plot  $\mathcal{C}_t(u_A)$  for some time  $t$ . Color a trivalent vertex black (respectively, white) if it has a unique edge extending downwards (respectively, upwards) from it. We preserve the labeling of regions and edges that was used in the contour plot: we label a region by  $E_I$  if the dominant exponential in that region is  $\Delta_I E_I$ , and label each line-soliton by its *type*  $[i, j]$  (see Lemma 5.5). We also preserve the topology of the graph, but forget the metric structure. We call this labeled graph with bicolored vertices the *soliton graph*  $G_{t_0}(u_A)$ .

*Example 7.2.* We continue Example 6.3. Figure 4 contains the same contour plot  $\mathcal{C}_t(u_A)$  as that at the left of Figure 3. One may use Lemma 5.5 to label all regions and edges in the soliton graph. After computing the Plücker coordinates, one can identify the singular solitons, which are indicated by the dotted lines in the soliton graph.

We now describe how to pass from a soliton graph to a *generalized plabic graph*.

*Definition 7.3.* A *generalized plabic graph* is an undirected graph  $G$  drawn inside a disk with  $n$  *boundary vertices* labeled  $\{1, \dots, n\}$ . We require that each boundary vertex  $i$  is either isolated (in which case it is colored with color 1 or  $-1$ ), or is incident to a single edge; and each internal vertex is colored black or white. Edges are allowed to cross each other in an  $X$ -crossing (which is not considered to be a vertex).

By Theorem 6.1, the following construction is well-defined.

*Definition 7.4.* Fix a positroid stratum  $\mathcal{S}_{\pi^\cdot}$  of  $Gr_{k,n}$  where  $\pi^\cdot = (\pi, \text{col})$ . To each soliton graph  $C$  coming from a point of that stratum we associate a generalized plabic graph  $Pl(C)$  by:

- embedding  $C$  into a disk, so that each unbounded line-soliton of  $C$  ends at a *boundary vertex*;
- labeling the boundary vertex incident to the edge with labels  $i$  and  $\pi(i)$  by  $\pi(i)$ ;
- adding an isolated boundary vertex labeled  $h$  with color 1 (respectively,  $-1$ ) whenever  $h \in J$  for each region label  $E_J$  (respectively, whenever  $h \notin J$  for any region label  $E_J$ );

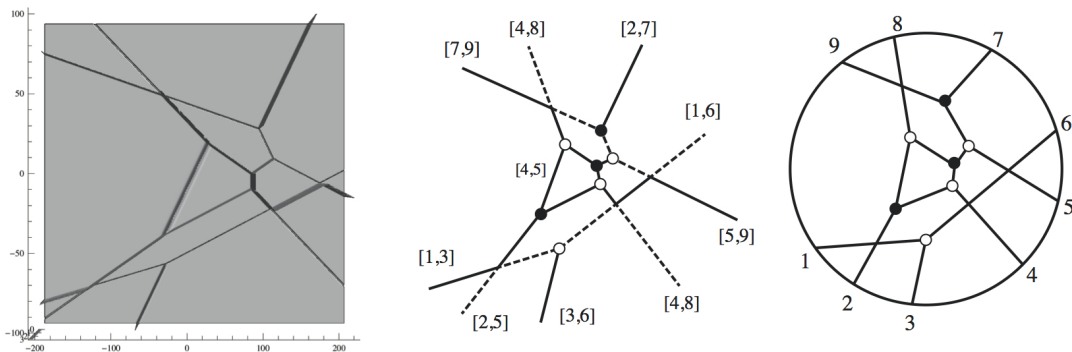


FIGURE 4. Example of a contour plot  $\mathcal{C}_t(u_A)$ , its soliton graph  $C = G_t(u_A)$ , and its generalized plabic graph  $Pl(C)$ . The parameters used are those from Example 6.3. In particular,  $(\kappa_1, \dots, \kappa_9) = (-5, -3, -2, -1, 0, 1, 2, 3, 4)$ , and  $\pi = (6, 7, 1, 8, 2, 3, 9, 4, 5)$ .

- forgetting the labels of all edges and regions.

See Figure 4 for a soliton graph  $C$  together with the corresponding generalized plabic graph  $Pl(C)$ .

*Definition 7.5.* Given a generalized plabic graph  $G$ , the *trip*  $T_i$  is the directed path which starts at the boundary vertex  $i$ , and follows the “rules of the road”: it turns right at a black vertex, left at a white vertex, and goes straight through the  $X$ -crossings. Note that  $T_i$  will also end at a boundary vertex. If  $i$  is an isolated vertex, then  $T_i$  starts and ends at  $i$ . Define  $\pi_G(i) = j$  whenever  $T_i$  ends at  $j$ . It is not hard to show that  $\pi_G$  is a permutation, which we call the *trip permutation*.

We use the trips to label the edges and regions of each generalized plabic graph.

*Definition 7.6.* Given a generalized plabic graph  $G$ , start at each non-isolated boundary vertex  $i$  and label every edge along trip  $T_i$  with  $i$ . Such a trip divides the disk containing  $G$  into two parts: the part to the left of  $T_i$ , and the part to the right. Place an  $i$  in every region which is to the left of  $T_i$ . If  $h$  is an isolated boundary vertex with color 1, put an  $h$  in every region of  $G$ . After repeating this procedure for each boundary vertex, each edge will be labeled by up to two numbers (between 1 and  $n$ ), and each region will be labeled by a collection of numbers. Two regions separated by an edge labeled by both  $i$  and  $j$  will have region labels  $S$  and  $(S \setminus \{i\}) \cup \{j\}$ . When an edge is labeled by two numbers  $i < j$ , we write  $[i, j]$  on that edge, or  $\{i, j\}$  or  $\{j, i\}$  if we do not wish to specify the order of  $i$  and  $j$ .

*Theorem 7.7.* [19, Theorem 7.6] Consider a soliton graph  $C = G_t(u_A)$  coming from a point  $A$  of a positroid stratum  $\mathcal{S}_{\pi^i}$ , where  $\pi^i = (\pi, col)$ . Then the trip permutation of  $Pl(C)$  is  $\pi$ , and by labeling edges of  $Pl(C)$  according to Definition 7.6, we will recover the original edge and region labels in  $C$ .

We invite the reader to verify Theorem 7.7 for the graphs in Figure 4.

*Remark 7.8.* By Theorem 7.7, we can identify each soliton graph  $C$  with its generalized plabic graph  $Pl(C)$ . From now on, we will often ignore the labels of edges and regions of a soliton graph, and simply record the labels on boundary vertices.

## 8. THE CONTOUR PLOT FOR $t \ll 0$

Consider a matroid stratum  $S_{\mathcal{M}}$  contained in the Deodhar component  $S_D$ , where  $D$  is the corresponding or Go-diagram. From Definition 5.1 it is clear that the contour plot associated to any  $A \in S_{\mathcal{M}}$  depends only on  $\mathcal{M}$ , not on  $A$ . In fact for  $t \ll 0$  a stronger statement is true – the contour plot for any  $A \in S_{\mathcal{M}} \subset S_D$  depends only on  $D$ , and not on  $\mathcal{M}$ . In this section we will explain how to use  $D$  to construct first a generalized plabic graph  $G_-(D)$ , and then the contour plot  $\mathcal{C}_t(\mathcal{M})$  for  $t \ll 0$ .

**8.1. Definition of the contour plot for  $t \ll 0$ .** Recall from (5.4) the definition of  $f_{\mathcal{M}}(x, y, t)$ . To understand how it behaves for  $t \ll 0$ , let us rescale everything by  $t$ . Define  $\bar{x} = \frac{x}{t}$  and  $\bar{y} = \frac{y}{t}$ , and set

$$\phi_i(\bar{x}, \bar{y}) = \kappa_i \bar{x} + \kappa_i^2 \bar{y} + \kappa_i^3,$$

that is,  $\kappa_i x + \kappa_i^2 y + \kappa_i^3 t = t \phi_i(\bar{x}, \bar{y})$ . Note that because  $t$  is negative,  $x$  and  $y$  have the opposite signs of  $\bar{x}$  and  $\bar{y}$ . This leads to the following definition of the contour plot for  $t \ll 0$ .

*Definition 8.1.* We define the contour plot  $\mathcal{C}_{-\infty}(\mathcal{M})$  to be the locus in  $\mathbb{R}^2$  where

$$\min_{J \in \mathcal{M}} \left\{ \sum_{i=1}^k \phi_{j_i}(\bar{x}, \bar{y}) \right\} \quad \text{is not linear .}$$

*Remark 8.2.* After a  $180^\circ$  rotation,  $\mathcal{C}_{-\infty}(\mathcal{M})$  is the limit of  $\mathcal{C}_t(u_A)$  as  $t \rightarrow -\infty$ , for any  $A \in S_{\mathcal{M}}$ . Note that the rotation is required because the positive  $x$ -axis (respectively,  $y$ -axis) corresponds to the negative  $\bar{x}$ -axis (respectively,  $\bar{y}$ -axis).

*Definition 8.3.* Define  $v_{i,\ell,m}$  to be the point in  $\mathbb{R}^2$  where  $\phi_i(\bar{x}, \bar{y}) = \phi_\ell(\bar{x}, \bar{y}) = \phi_m(\bar{x}, \bar{y})$ . A simple calculation yields that the point  $v_{i,\ell,m}$  has the following coordinates in the  $\bar{x}\bar{y}$ -plane:

$$v_{i,\ell,m} = (\kappa_i \kappa_\ell + \kappa_i \kappa_m + \kappa_\ell \kappa_m, -(\kappa_i + \kappa_\ell + \kappa_m)).$$

Some of the points  $v_{i,\ell,m} \in \mathbb{R}^2$  correspond to trivalent vertices in the contour plots we construct; such a point is the location of the resonant interaction of three line-solitons of types  $[i, \ell]$ ,  $[\ell, m]$  and  $[i, m]$  (see Theorem 8.5 below). Because of our assumption on the genericity of the  $\kappa$ -parameters, those points are all distinct.

**8.2. Main results on the contour plot for  $t \ll 0$ .** This section is based on [20, Section 10], and generalizes the results of [19, Section 8] to a soliton solution coming from an arbitrary point of the real Grassmannian (not just the non-negative part). We start by giving an algorithm to construct a generalized plabic graph  $G_-(D)$ , which will be used to construct  $\mathcal{C}_{-\infty}(\mathcal{M})$ . Figure 5 illustrates the steps of Algorithm 8.4, starting from the Go-diagram of the Deodhar component  $S_D$  where  $D$  is as in the upper left corner of Figure 5.

*Algorithm 8.4.* [20, Algorithm 10.4] From a Go-diagram  $D$  to  $G_-(D)$ :

- (1) Start with a Go-diagram  $D$  contained in a  $k \times (n - k)$  rectangle, and replace each  $\circ$ ,  $\bullet$ , and blank box by a cross, a cross, and a pair of *elbows*, respectively. Label the  $n$  edges along the southeast border of the Young diagram by the numbers 1 to  $n$ , from northeast to southwest. The configuration of crosses and elbows forms  $n$  “pipes” which travel from the southeast border to the northwest border; label the endpoint of each pipe by the label of its starting point.
- (2) Add a pair of black and white vertices to each pair of elbows, and connect them by an edge, as shown in the upper right of Figure 5. Forget the labels of the southeast border. If there is an endpoint of a pipe on the east or south border whose pipe starts by going straight, then erase the straight portion preceding the first elbow. If there is a horizontal (respectively, vertical) pipe starting at  $i$  with no elbows, then erase it, and add an isolated boundary vertex labeled  $i$  with color 1 (respectively,  $-1$ ).
- (3) Forget any degree 2 vertices, and forget any edges of the graph which end at the southeast border of the diagram. Denote the resulting graph  $G_-(D)$ .
- (4) After embedding the graph in a disk with  $n$  boundary vertices (including isolated vertices) we obtain a generalized plabic graph, which we also denote  $G_-(D)$ . If desired, stretch and rotate  $G_-(D)$  so that the boundary vertices at the west side of the diagram are at the north instead.

The following is the main result of this section.

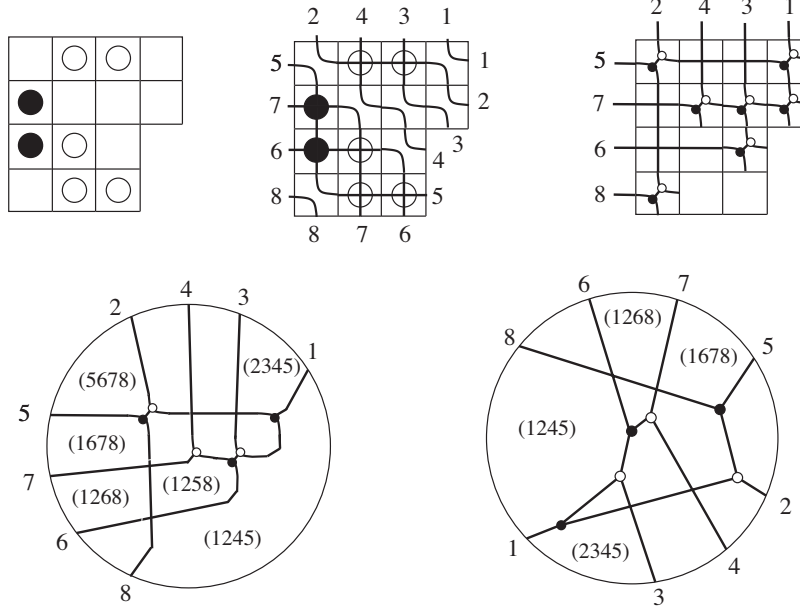


FIGURE 5. Construction of the generalized plabic graph  $G_-(D)$  associated to the Go-diagram  $D$ . The labels of the regions of the graph indicate the index sets of the corresponding Plücker coordinates. Using the notation of Definition 4.7, we have  $\pi(D) = vw^{-1} = (5, 7, 1, 6, 8, 3, 4, 2)$ .

*Theorem 8.5.* [20, Theorem 10.6] Choose a matroid stratum  $S_{\mathcal{M}}$  and let  $S_D$  be the Deodhar component containing  $S_{\mathcal{M}}$ . Recall the definition of  $\pi(D)$  from Definition 4.7. Use Algorithm 8.4 to obtain  $G_-(D)$ . Then  $G_-(D)$  has trip permutation  $\pi(D)$ , and we can use it to explicitly construct  $\mathcal{C}_{-\infty}(\mathcal{M})$  as follows. Label the edges of  $G_-(D)$  according to the rules of the road. Label by  $v_{i,\ell,m}$  each trivalent vertex which is incident to edges labeled  $[i,\ell]$ ,  $[i,m]$ , and  $[\ell,m]$ , and give that vertex the coordinates  $(\bar{x}, \bar{y}) = (\kappa_i\kappa_\ell + \kappa_i\kappa_m + \kappa_\ell\kappa_m, -(\kappa_i + \kappa_\ell + \kappa_m))$ . Replace each edge labeled  $[i,j]$  which ends at a boundary vertex by an unbounded line-soliton with slope  $\kappa_i + \kappa_j$ . (Each edge labeled  $[i,j]$  between two trivalent vertices will automatically have slope  $\kappa_i + \kappa_j$ .) In particular,  $\mathcal{C}_{-\infty}(\mathcal{M})$  is determined by  $D$ . Recall from Remark 8.2 that after a  $180^\circ$  rotation,  $\mathcal{C}_{-\infty}(\mathcal{M})$  is the limit of  $\mathcal{C}_t(u_A)$  as  $t \rightarrow -\infty$ , for any  $A \in S_{\mathcal{M}}$ .

*Remark 8.6.* Since the contour plot  $\mathcal{C}_{-\infty}(\mathcal{M})$  depends only on  $D$ , we also refer to it as  $\mathcal{C}_{-\infty}(D)$ .

*Remark 8.7.* The results of this section may be extended to the case  $t \gg 0$  by duality considerations (similar to the way in which our previous paper [19] described contour plots for both  $t \ll 0$  and  $t \gg 0$ ). Note that the Deodhar decomposition of  $Gr_{k,n}$  depends on a choice of ordered basis  $(e_1, \dots, e_n)$ . Using the ordered basis  $(e_n, \dots, e_1)$  instead and the corresponding Deodhar decomposition, one may explicitly describe contour plots at  $t \gg 0$ .

*Remark 8.8.* Depending on the choice of the parameters  $\kappa_i$ , the contour plot  $\mathcal{C}_{-\infty}(D)$  may have a slightly different topological structure than the soliton graph  $G_-(D)$ . While the incidences of line-solitons with trivalent vertices are determined by  $G_-(D)$ , the locations of  $X$ -crossings may vary based on the  $\kappa_i$ 's. More specifically, changing the  $\kappa_i$ 's may change the contour plot via a sequence of *slides*, see [20, Section 11].

**8.3.  $X$ -crossings in the contour plots.** Recall the notions of black and white  $X$ -crossings from Definition 5.7. In [19, Theorem 9.1], we proved that the presence of  $X$ -crossings in contour plots at  $|t| \gg 0$  implies that there is a two-term Plücker relation.

*Theorem 8.9.* [19, Theorem 9.1] Suppose that there is an  $X$ -crossing in a contour plot  $\mathcal{C}_t(u_A)$  for some  $A \in Gr_{k,n}$  where  $|t| \gg 0$ . Let  $I_1, I_2, I_3$ , and  $I_4$  be the  $k$ -element subsets of  $\{1, \dots, n\}$  corresponding to the dominant exponentials incident to the  $X$ -crossing listed in circular order.

- If the  $X$ -crossing is white, we have  $\Delta_{I_1}(A)\Delta_{I_3}(A) = \Delta_{I_2}(A)\Delta_{I_4}(A)$ .
- If the  $X$ -crossing is black, we have  $\Delta_{I_1}(A)\Delta_{I_3}(A) = -\Delta_{I_2}(A)\Delta_{I_4}(A)$ .

The following corollary is immediate.

*Corollary 8.10.* If there is a black  $X$ -crossing in a contour plot at  $t \ll 0$  or  $t \gg 0$ , then among the Plücker coordinates associated to the dominant exponentials incident to that black  $X$ -crossing, three must be positive and one negative, or vice-versa.

*Corollary 8.11.* Let  $D$  be a  $\mathbb{J}$ -diagram, that is, a Go-diagram with no black stones. Let  $A \in S_D$  and  $t \ll 0$ . Choose any  $\kappa_1 < \dots < \kappa_n$ . Then the contour plot  $\mathcal{C}_t(u_A)$  can have only white  $X$ -crossings.

## 9. TOTAL POSITIVITY, REGULARITY, AND CLUSTER ALGEBRAS

In this paper we have been studying solutions  $u_A(x, y, t)$  to the KP equation coming from points of the real Grassmannian. Among these solutions, those coming from the totally non-negative part of  $Gr_{k,n}$  are especially nice. In particular,  $(Gr_{k,n})_{\geq 0}$  parameterizes the *regular* soliton solutions coming from  $Gr_{k,n}$ , see Theorem 9.1. This result provides an important motivation for studying the soliton solutions coming from  $(Gr_{k,n})_{\geq 0}$ . After discussing the regularity result below, we will discuss *positivity tests* for elements of the Grassmannian, as well as the connection between soliton solutions from  $(Gr_{k,n})_{> 0}$  and the theory of cluster algebras.

*Theorem 9.1.* [20, Theorem 12.1] Fix parameters  $\kappa_1 < \dots < \kappa_n$  and an element  $A \in Gr_{k,n}$ . Consider the corresponding soliton solution  $u_A(x, y, t)$  of the KP equation. This solution is regular at  $t \ll 0$  if and only if  $A \in (Gr_{k,n})_{\geq 0}$ . Therefore this solution is regular for all times  $t$  if and only if  $A \in (Gr_{k,n})_{\geq 0}$ .

If one is studying total positivity on the Grassmannian, then a natural question is the following: given  $A \in Gr_{k,n}$ , how many Plücker coordinates, and which ones, must one compute, in order to determine that  $A \in (Gr_{k,n})_{\geq 0}$ ? This leads to the following notion of *positivity test*.

*Definition 9.2.* Consider the Deodhar component  $S_D \subset Gr_{k,n}$ , where  $D$  is a Go-diagram. A collection  $\mathcal{J}$  of  $k$ -element subsets of  $\{1, 2, \dots, n\}$  is called a *positivity test* for  $S_D$  if for any  $A \in S_D$ , the condition that  $\Delta_I(A) > 0$  for all  $I \in \mathcal{J}$  implies that  $A \in (Gr_{k,n})_{\geq 0}$ .

It turns out that the collection of Plücker coordinates corresponding to dominant exponentials in contour plots at  $t \ll 0$  provide positivity tests for positroid strata.

*Theorem 9.3.* [20, Theorem 12.9] Let  $A \in S_D \subset Gr_{k,n}$ , where  $D$  is a  $\mathbb{J}$ -diagram, and let  $t \ll 0$ . If  $\Delta_J(A) > 0$  for each dominant exponential  $E_J$  in the contour plot  $\mathcal{C}_t(u_A)$ , then  $A \in (Gr_{k,n})_{\geq 0}$ . In other words, the Plücker coordinates corresponding to the dominant exponentials in  $\mathcal{C}_t(u_A)$  comprise a positivity test for  $S_D$ .

*Remark 9.4.* Recall that the Deodhar components  $S_D$  have non-empty intersection with  $(Gr_{k,n})_{\geq 0}$  unless  $D$  is a  $\mathbb{J}$ -diagram. Therefore Theorem 9.3 restricts to the case that  $D$  is a  $\mathbb{J}$ -diagram.

**9.1. TP Schubert cells and reduced plabic graphs.** In this section we provide a new characterization of the so-called *reduced* plabic graphs [25, Section 12]. This will allow us to make a connection to cluster algebras in Section 9.2.

We will always assume that a plabic graph is *leafless*, i.e. that it has no non-boundary leaves, and that it has no isolated components. In order to define *reduced*, we first define some local transformations of plabic graphs.

(M1) **SQUARE MOVE.** If a plabic graph has a square formed by four trivalent vertices whose colors alternate, then we can switch the colors of these four vertices.

(M2) **UNICOLORED EDGE CONTRACTION/UNCONTRACTION.** If a plabic graph contains an edge with two vertices of the same color, then we can contract this edge into a single vertex with the same color. We can also uncontract a vertex into an edge with vertices of the same color.

(M3) **MIDDLE VERTEX INSERTION/REMOVAL.** If a plabic graph contains a vertex of degree 2, then we can remove this vertex and glue the incident edges together; on the other hand, we can always insert a vertex (of any color) in the middle of any edge.

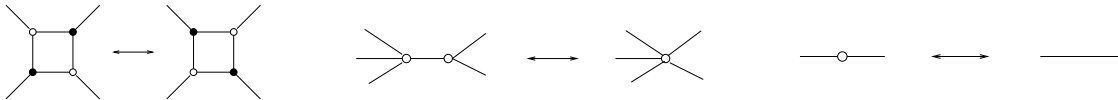


FIGURE 6. A square move; a unicolored edge contraction; a middle vertex insertion/ removal

(R1) **PARALLEL EDGE REDUCTION.** If a network contains two trivalent vertices of different colors connected by a pair of parallel edges, then we can remove these vertices and edges, and glue the remaining pair of edges together.

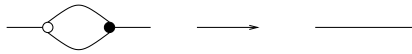


FIGURE 7. Parallel edge reduction

*Definition 9.5.* [25] Two plabic graphs are called *move-equivalent* if they can be obtained from each other by moves (M1)-(M3). The *move-equivalence class* of a given plabic graph  $G$  is the set of all plabic graphs which are move-equivalent to  $G$ . A leafless plabic graph without isolated components is called *reduced* if there is no graph in its move-equivalence class to which we can apply (R1).

*Theorem 9.6.* [25, Theorem 13.4] Two reduced plabic graphs which each have  $n$  boundary vertices are move-equivalent if and only if they have the same trip permutation.

Our new characterization of reduced plabic graphs is as follows.

*Definition 9.7.* We say that a (generalized) plabic graph has the *resonance property*, if after labeling edges via Definition 7.6, the set  $E$  of edges incident to a given vertex has the following property:

- there exist numbers  $i_1 < i_2 < \dots < i_m$  such that when we read the labels of  $E$ , we see the labels  $[i_1, i_2], [i_2, i_3], \dots, [i_{m-1}, i_m], [i_1, i_m]$  appear in counterclockwise order.

*Theorem 9.8.* [19, Theorem 10.5]. A plabic graph is reduced if and only if it has the resonance property.<sup>6</sup>

*Corollary 9.9.* [19, Corollary 10.9] Suppose that  $A$  lies in a TP Schubert cell, and that for some time  $t$ ,  $G_t(u_A)$  is generic with no X-crossings. Then  $G_t(u_A)$  is a reduced plabic graph.

<sup>6</sup>Recall from Definition 2.11 that our convention is to label boundary vertices of a plabic graph  $1, 2, \dots, n$  in counterclockwise order. If one chooses the opposite convention, then one must replace the word *counterclockwise* in Definition 9.7 by *clockwise*.

**9.2. The connection to cluster algebras.** Cluster algebras are a class of commutative rings, introduced by Fomin and Zelevinsky [10], which have a remarkable combinatorial structure. Many coordinate rings of homogeneous spaces have a cluster algebra structure: as shown by Scott [28], the Grassmannian is one such example.

*Theorem 9.10.* [28] The coordinate ring of (the affine cone over)  $Gr_{k,n}$  has a cluster algebra structure. Moreover, the set of Plücker coordinates whose indices come from the labels of the regions of a reduced plabic graph for  $(Gr_{k,n})_{>0}$  comprises a *cluster* for this cluster algebra.

*Remark 9.11.* In fact [28] used the combinatorics of *alternating strand diagrams*, not reduced plabic graphs, to describe clusters. However, alternating strand diagrams are in bijection with reduced plabic graphs [25].

*Theorem 9.12.* [19, 10.12] The set of Plücker coordinates labeling regions of a generic trivalent soliton graph for the TP Grassmannian is a cluster for the cluster algebra associated to the Grassmannian.

Conjecturally, every positroid cell  $\mathcal{S}_\pi^{tnn}$  of the totally non-negative Grassmannian also carries a cluster algebra structure, and the Plücker coordinates labeling the regions of any reduced plabic graph for  $\mathcal{S}_\pi^{tnn}$  should be a cluster for that cluster algebra. In particular, the TP Schubert cells should carry cluster algebra structures. Therefore we conjecture that Theorem 9.12 holds with “Schubert cell” replacing “Grassmannian.” Finally, there should be a suitable generalization of Theorem 9.12 for arbitrary positroid cells.

**9.3. Soliton graphs for  $(Gr_{2,n})_{>0}$  and triangulations of an  $n$ -gon.** In this section we must use a slightly more general setup for  $\tau$ -functions  $\tau_A(t_1, \dots, t_m)$  and soliton solutions  $u_A(t_1, \dots, t_m)$ , in which the exponential functions  $E_i$  and  $E_I$  are functions of variables  $t_1, \dots, t_m$ , and  $m \geq n$ . Here  $t_1 = x$ ,  $t_2 = y$ ,  $t_3 = t$ , and the other  $t_i$ 's are referred to as *higher times*. See [19, Section 3] for details.

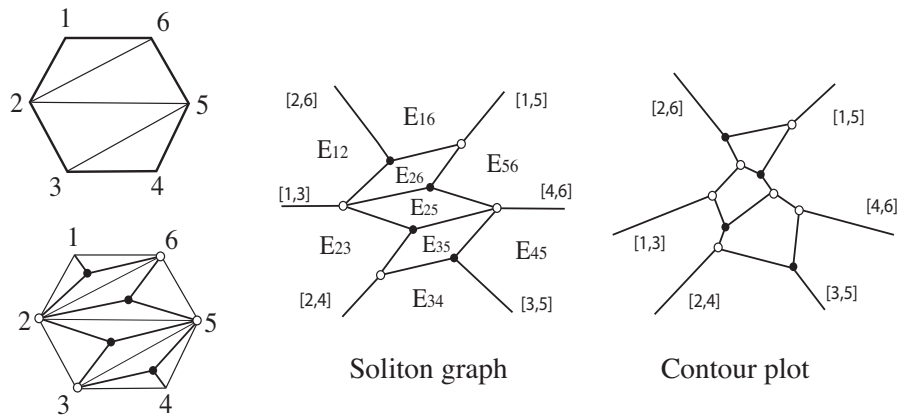


FIGURE 8. Algorithm 9.13, starting from a triangulation of a hexagon. The right figure shows the corresponding contour plot for the soliton solution for  $(Gr_{2,6})_{>0}$ .

*Algorithm 9.13.* [19, Algorithm 12.1] Let  $T$  be a triangulation of an  $n$ -gon  $P$ , whose  $n$  vertices are labeled by the numbers  $1, 2, \dots, n$ , in counterclockwise order. Therefore each edge of  $P$  and each diagonal of  $T$  is specified by a pair of distinct integers between 1 and  $n$ . The following procedure yields a labeled graph  $\Psi(T)$ .

- (1) Put a black vertex in the interior of each triangle in  $T$ .

- (2) Put a white vertex at each of the  $n$  vertices of  $P$  which is incident to a diagonal of  $T$ ; put a black vertex at the remaining vertices of  $P$ .
- (3) Connect each vertex which is inside a triangle of  $T$  to the three vertices of that triangle.
- (4) Erase the edges of  $T$ , and contract every pair of adjacent vertices which have the same color. This produces a new graph  $G$  with  $n$  boundary vertices, in bijection with the vertices of the original  $n$ -gon  $P$ .
- (5) Add one unbounded ray to each of the boundary vertices of  $G$ , so as to produce a new (planar) graph  $\Psi(T)$ . Note that  $\Psi(T)$  divides the plane into regions; the bounded regions correspond to the diagonals of  $T$ , and the unbounded regions correspond to the edges of  $P$ .

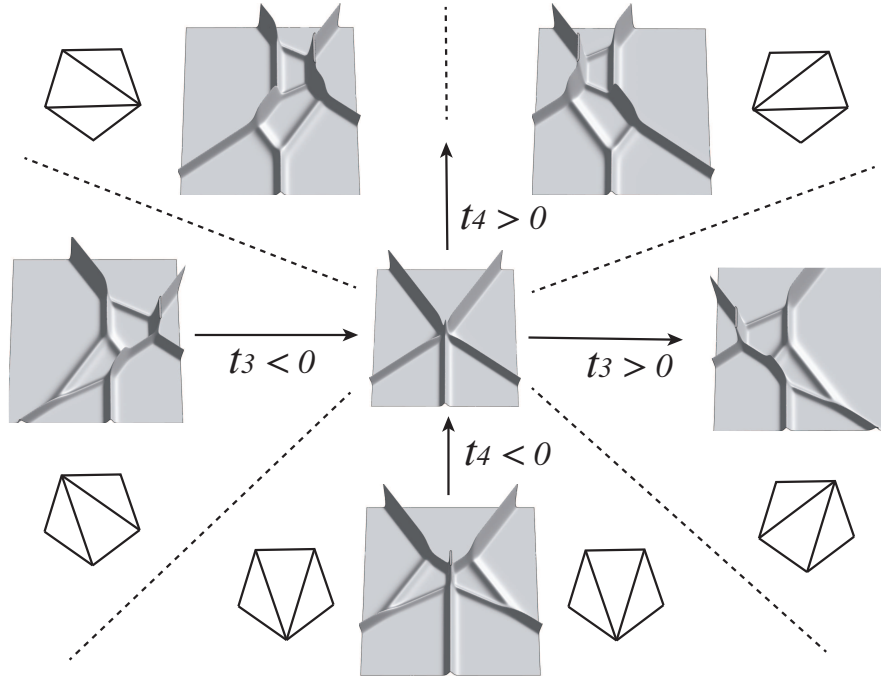


FIGURE 9. Contour plots corresponding to the different soliton graphs for  $(Gr_{2,5})_{>0}$ . The center figure shows the contour plot at  $t_3 = t_4 = 0$ .

See Figure 8. Our main result in this section is the following.

*Theorem 9.14.* [19, Theorem 12.1] The graphs  $\Psi(T)$  constructed above *are* soliton graphs for  $(Gr_{2,n})_{>0}$ , and conversely, up to (M2)-equivalence, any trivalent generic soliton graph for  $(Gr_{2,n})_{>0}$  comes from this construction. Moreover, one can realize each graph  $\Psi(T)$  by either:

- choosing an arbitrary  $A \in (Gr_{2,n})_{>0}$  and varying the higher times  $t_3, \dots, t_n$  appropriately, or
- fixing an arbitrary collection of higher times  $t_3, \dots, t_n$ , and using the torus action to choose an appropriate  $A \in (Gr_{2,n})_{>0}$ .

Figure 9 shows the five triangulations of a pentagon, together with (contour plots corresponding to) the five different soliton graphs which one may obtain from  $(Gr_{2,5})_{>0}$ .

*Remark 9.15.* The process of flipping a diagonal in the triangulation corresponds to a mutation in the cluster algebra. In the terminology of reduced plabic graphs, a mutation corresponds to the square



move (M1). In the setting of KP solitons, each mutation may be considered as an evolution along a particular flow of the KP hierarchy defined by the symmetries of the KP equation.

*Remark 9.16.* It is known already that the set of reduced plabic graphs for the TP part of  $Gr_{2,n}$  all have the form given by Algorithm 9.13. And by Corollary 9.9, every generic soliton graph is a reduced plabic graph. Therefore it follows immediately that every soliton graph for the TP part of  $Gr_{2,n}$  must have the form of Algorithm 9.13. To prove Theorem 9.14, one must also show that every outcome of Algorithm 9.13 can be realized as a soliton graph.

## 10. THE INVERSE PROBLEM FOR SOLITON GRAPHS

The *inverse* problem for soliton solutions of the KP equation is the following: given a time  $t$  together with the contour plot  $\mathcal{C}_t(u_A)$  of a soliton solution, can one reconstruct the point  $A$  of  $Gr_{k,n}$  which gave rise to the solution? Note that solving for  $A$  is desirable, because this information would allow us to compute the entire past and the entire future of the soliton solution.

Using the cluster algebra structure for Grassmannians, we have the following.

*Theorem 10.1.* [19, Theorem 11.2] Consider a generic contour plot  $\mathcal{C}_t(u_A)$  of a soliton solution which has no  $X$ -crossings, and which comes from a point  $A$  of the totally positive Grassmannian at an *arbitrary* time  $t$ . Then from the contour plot together with  $t$  we can uniquely reconstruct the point  $A$ .

Using the description of contour plots of soliton solutions when  $t \ll 0$ , we have the following.

*Theorem 10.2.* [19, Theorem 11.3] Fix  $\kappa_1 < \dots < \kappa_n$  as usual. Consider a generic contour plot  $\mathcal{C}_t(u_A)$  of a soliton solution coming from a point  $A$  of a positroid cell  $S_\pi^{tnn}$ , for  $t \ll 0$ . Then from the contour plot together with  $t$  we can uniquely reconstruct the point  $A$ .

**10.1. Non-uniqueness of the evolution of the contour plots for  $t \gg 0$ .** In contrast to the totally non-negative case, where the soliton solution can be uniquely determined by the information in the contour plot at  $t \ll 0$ , if we consider arbitrary points  $A \in Gr_{k,n}$ , we cannot solve the inverse problem.

Consider  $A \in S_D \subset Gr_{k,n}$ . If the contour plot  $\mathcal{C}_{-\infty}(D)$  is topologically identical to  $G_-(D)$ , then the contour plot has almost no dependence on the parameters  $m_j$  from the parameterization of  $S_D$ . This is because the Plücker coordinates corresponding to the regions of  $\mathcal{C}_{-\infty}(D)$  (representing the dominant exponentials) are either monomials in the  $p_i$ 's (see [19, Section 5] and [19, Remark 10.5]), or determined from these by a “two-term” Plücker relation.

Therefore it is possible to choose two different points  $A$  and  $A'$  in  $S_D \subset Gr_{k,n}$  whose contour plots for a fixed  $\kappa_1 < \dots < \kappa_n$  and fixed  $t \ll 0$  are identical (up to some exponentially small difference); we use the same parameters  $p_i$  but different parameters  $m_j$  for defining  $A$  and  $A'$ . However, as  $t$  increases, those contour plots may evolve to give different patterns.

Consider the Deodhar stratum  $S_D \subset Gr_{2,4}$ , corresponding to

$$\mathbf{w} = s_2 s_3 s_1 s_2 \text{ and } \mathbf{v} = s_2 1 1 s_2.$$

The Go-diagram and labeled Go-diagram are given by

$$\begin{array}{|c|c|} \hline \bullet & \\ \hline & \circ \\ \hline \end{array} \quad \begin{array}{|c|c|} \hline -1 & p_3 \\ \hline p_2 & 1 \\ \hline \end{array}.$$

The matrix  $g$  is calculated as  $g = s_2 y_3(p_2) y_1(p_3) x_2(m) s_2^{-1}$ , and its projection to  $Gr_{2,4}$  is

$$A = \begin{pmatrix} -p_3 & -m & 1 & 0 \\ 0 & p_2 & 0 & 1 \end{pmatrix}.$$

The  $\tau$ -function is

$$\tau_A = -(p_2 p_3 E_{1,2} + p_3 E_{1,4} + m E_{2,4} + p_2 E_{2,3} - E_{3,4}),$$

where  $E_{i,j} := (\kappa_j - \kappa_i) \exp(\theta_i + \theta_j)$ . The contour plots of the solutions with  $m = 0$  and  $m \neq 0$  are the same (except for some exponentially small difference) when  $t \ll 0$ . In both cases, the plot consists of two line-solitons forming an  $X$ -crossing, where the parts of those solitons adjacent to the region with dominant exponential  $E_{3,4}$  (i.e. for  $x \gg 0$ ) are singular, see the left of Figure 10.

On the other hand, for  $t \gg 0$ , the contour plot with  $m = 0$  is topologically the same as it was for  $t \ll 0$ , while the contour plot with  $m \neq 0$  has a box with dominant exponential  $E_{2,4}$ , surrounded by four bounded solitons (some of which are singular). See the middle and right of Figure 10. So not only the contour plots but also the soliton graphs are different for  $t \gg 0$ !

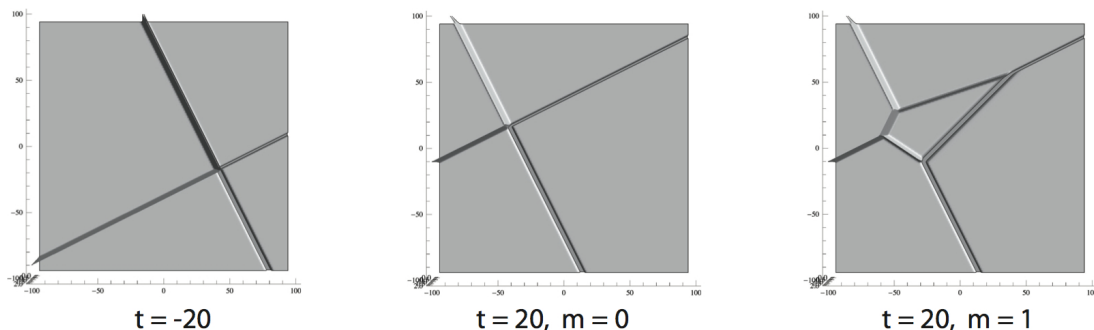


FIGURE 10. The non-uniqueness of the evolution of the contour plots (and soliton graphs). The left panel shows the contour plot at  $t = -20$  for any value of  $m$ . The middle panel shows the graph at  $t = 20$  with  $m = 0$ , and the right one shows the graph at  $t = 20$  with  $m = 1$ . These contour plots were made using the choice  $p_i = 1$  for all  $i$ , and  $(\kappa_1, \dots, \kappa_4) = (-2, -1, 0, 1.5)$ . In all of them, the region at  $x \gg 0$  has a positive sign ( $\Delta_{3,4} = 1$ ) and other regions have negative signs. This means that the solitons adjacent to the region for  $x \gg 0$  are singular.

Note that the non-uniqueness of the evolution of the contour plot (a tropical approximation) does not imply the non-uniqueness of the evolution of the solution of the KP equation as  $t$  changes. If one makes two different choices for the  $m_i$ 's, the corresponding  $\tau$ -functions are different, but there is only an exponentially small difference in the corresponding contour plots (hence the topology of the contour plots is identical).

## REFERENCES

- [1] M. J. Ablowitz and P. A. Clarkson, *Solitons, nonlinear evolution equations and inverse scattering* (Cambridge University Press, Cambridge, 1991)
- [2] G. Biondini and S. Chakravarty, Soliton solutions of the Kadomtsev-Petviashvili II equation, *J. Math. Phys.*, **47** (2006) 033514 (26pp).
- [3] G. Biondini, Y. Kodama, On a family of solutions of the Kadomtsev-Petviashvili equation which also satisfy the Toda lattice hierarchy, *J. Phys. A: Math. Gen.* **36** (2003), 10519–10536.
- [4] A. Bjorner and F. Brenti, *Combinatorics of Coxeter groups*, Graduate Texts in Mathematics, 231, Springer, New York, 2005.
- [5] S. Chakravarty, Y. Kodama, Classification of the line-solitons of KP II, *J. Phys. A: Math. Theor.* **41** (2008) 275209 (33pp).
- [6] S. Chakravarty, Y. Kodama, A generating function for the N-soliton solutions of the Kadomtsev-Petviashvili II equation, *Contemp. Math.*, **471** (2008), 47–67.

- [7] S. Chakravarty, Y. Kodama, Soliton solutions of the KP equation and applications to shallow water waves, *Stud. Appl. Math.* **123** (2009) 83–151.
- [8] V. Deodhar, On some geometric aspects of Bruhat orderings. I. A finer decomposition of Bruhat cells, *Invent. Math.* **79** (1985), no. 3, 499–511.
- [9] L. A. Dickey, *Soliton equations and Hamiltonian systems*, Advanced Series in Mathematical Physics, Vol. **12**, (World Scientific, Singapore, 1991).
- [10] S. Fomin, A. Zelevinsky, Cluster Algebras I: Foundations, *J. Amer. Math. Soc.* **15** (2002), 497–529.
- [11] N. Freeman, J. Nimmo, Soliton-solutions of the Korteweg-deVries and Kadomtsev-Petviashvili equations: the Wronskian technique, *Phys. Lett. A* **95** (1983), 1–3.
- [12] R. Hirota, *The Direct Method in Soliton Theory* (Cambridge University Press, Cambridge, 2004)
- [13] B. B. Kadomtsev and V. I. Petviashvili, On the stability of solitary waves in weakly dispersive media, *Sov. Phys. - Dokl.* **15** (1970) 539–541.
- [14] D. Kazhdan and G. Lusztig, Representations of Coxeter groups and Hecke algebras, *Invent. Math.* **53** (1979), no. 2, 165–184.
- [15] D. Kazhdan and G. Lusztig, *Schubert varieties and Poincaré duality*, Geometry of the Laplace operator (Proc. Sympos. Pure Math., Univ. Hawaii, Honolulu, Hawaii, 1979), Proc. Sympos. Pure Math., XXXVI, Amer. Math. Soc., Providence, R.I., 1980, pp. 185–203. MR 84g:14054
- [16] Y. Kodama, Young diagrams and  $N$ -soliton solutions of the KP equation, *J. Phys. A: Math. Gen.*, **37** (2004) 11169–11190.
- [17] Y. Kodama, KP solitons in shallow water, *J. Phys. A: Math. Theor.* **43** (2010) 434004 (54pp).
- [18] Y. Kodama, L. Williams, KP solitons, total positivity, and cluster algebras, *Proc. Natl. Acad. Sci. USA* **108** (2011), no. 22, 8984–8989.
- [19] Y. Kodama, L. Williams, KP solitons and total positivity for the Grassmannian, [arXiv:1106.0023](https://arxiv.org/abs/1106.0023).
- [20] Y. Kodama, L. Williams, A Deodhar decomposition of the Grassmannian and the regularity of KP solitons, [arXiv:1204.6446](https://arxiv.org/abs/1204.6446).
- [21] G. Lusztig, Total positivity in partial flag manifolds, *Representation Theory*, **2** (1998) 70–78.
- [22] R. Marsh and K. Rietsch, Parametrizations of flag varieties, *Representation Theory*, **8** (2004).
- [23] T. Miwa and M. Jimbo and E. Date, *Solitons: differential equations, symmetries and infinite-dimensional algebras* (Cambridge University Press, Cambridge, 2000)
- [24] S. Novikov, S. V. Manakov, L. P. Pitaevskii and V. E. Zakharov, *Theory of Solitons: The Inverse Scattering Method*, Contemporary Soviet Mathematics, (Consultants Bureau, New York and London, 1984).
- [25] A. Postnikov, Total positivity, Grassmannians, and networks, <http://front.math.ucdavis.edu/math.CO/0609764>.
- [26] M. Sato, Soliton equations as dynamical systems on an infinite dimensional Grassmannian manifold, *RIMS Kokyuroku* (Kyoto University) **439** (1981), 30–46.
- [27] J. Satsuma, A Wronskian representation of  $N$ -soliton solutions of nonlinear evolution equations, *J. Phys. Soc. Japan*, **46** (1979) 356–360.
- [28] J. Scott, Grassmannians and cluster algebras, *Proc. London Math. Soc.* (3) **92** (2006), 345–380.
- [29] J. Stembridge, On the Fully Commutative Elements of Coxeter Groups. *J. Algebraic Combinatorics* **5** (1996), 353–385.

DEPARTMENT OF MATHEMATICS, OHIO STATE UNIVERSITY, COLUMBUS, OH 43210

*E-mail address:* [kodama@math.ohio-state.edu](mailto:kodama@math.ohio-state.edu)

DEPARTMENT OF MATHEMATICS, UNIVERSITY OF CALIFORNIA, BERKELEY, CA 94720-3840

*E-mail address:* [williams@math.berkeley.edu](mailto:williams@math.berkeley.edu)